

1 **Description of changes made to ‘Attribution of sea ice model biases to specific model**
2 **errors enabled by new induced surface flux framework’**

3

4 In this document, changes made to the manuscript arising from the reviews are described.
5 The original point-by-point response to the reviews, and a version of the manuscript with
6 changes tracked, are appended.

7

8 **1. Fundamental changes to the analysis**

9 In response to a suggestion by Reviewer 2, fields of surface flux estimated by the formulae
10 described in Section 2.3 of the original paper were compared to modelled actual surface flux
11 fields. While the estimated fields captured well the seasonal and spatial variation in surface
12 flux, large discrepancies in the absolute values were apparent (30-40 Wm^{-2} in some
13 months). As a result of these, the methods of estimating surface flux were refined in the
14 following ways:

- 15 • Surface flux contributions were estimated for each ice thickness category separately,
16 and then summed (as opposed to using the mean ice thickness across all
17 categories);
- 18 • The reference temperature about which the Stefan-Boltzmann relation is linearised
19 was allowed to vary in space and time (it was previously uniformly 0°C). For each
20 grid cell, this reference temperature was set to the monthly mean surface
21 temperature.
- 22 • A representation of the turbulent fluxes was added to the formulae.

23 The biases in estimated surface flux were greatly reduced by this method. The remaining
24 biases, and their implication for the results, are discussed in the new Appendix A, which
25 examines potential errors in the induced surface flux analysis.

26 Although the results of the analysis were not qualitatively changed by the new methods, the
27 contribution of the ice thickness bias during the winter to the surface flux bias was somewhat
28 increased, probably because the greater efficiency of ice production for thin ice is captured
29 more effectively by using the full thickness category information.

30 Because the new surface flux formulae use much more detailed information about the model
31 diagnostics, the approach of calculating surface flux dependency on each variable has
32 changed. Whereas in the previous version, the model-observation mean was used to
33 calculate partial derivatives (i.e. surface flux dependency on variable), in the new version only
34 the model state is used to calculate this. Implications of this are also discussed in the new
35 Appendix A.

36

37 **2. Major additions and corrections by section**

38 The structure of the paper has been altered slightly. The description of the induced surface
39 flux (ISF) analysis has been moved later in the paper, to a new Section 4, after the model
40 sea ice and surface radiation evaluation in Section 3. The derivation of the formulae is now
41 described briefly within this section, rather than in an appendix. Hence the new structure is

1 1 – Introduction

2 2 – Model and observational data description

3 3 – Sea ice and surface radiation evaluation

4 4 – ISF method description

5 5 – ISF results

6 6 – Discussion

7 7 – Conclusion

8 Appendix A – Discussion of ISF errors

9 Below, major additions and corrections are described section by section (minor corrections
10 are summarised in Section 3 of this document).

11

12 **2.1 Abstract and introduction**

13 In these sections, the presentation of the logic behind the ISF method has been altered, in
14 part inspired by the changes described in Section 1 above. It is hoped that as a result the
15 presentation is improved and clarified.

16 The argument is stated again here for ease of reading: at any model point in space and time,
17 we approximate model surface flux as a function of climate variables that affect the surface
18 flux on timescales shorter than that on which they affect each other. In this way, by taking
19 partial derivatives, we characterise at each point in space and time the rate at which surface
20 flux depends on any climate variable. Multiplication of the resulting field by an estimate of
21 model bias in that variable therefore produces a field of estimated surface flux bias induced
22 (on a near-instantaneous timescale) by the model bias in that variable. These fields can be
23 averaged in space and time to give large-scale estimates of surface flux bias, bypassing
24 nonlinearities present in the relationship between surface flux and climate variable. This
25 allows the proximate causes of surface flux bias (and hence bias in sea ice growth and melt)
26 to be directly quantified.

27 The argument above is presented fully in the new Section 4, but is summarised in the
28 Introduction, and more briefly summarised in the abstract. It is stated more carefully that the
29 ISF method can diagnose only proximate causes of surface flux bias, as pointed out by
30 Reviewer 1.

31

32 **2.2 Model and observational data**

33 In the model description, the sub-gridscale thickness distribution of HadGEM2-ES is now
34 described more carefully, as it is now key to the analysis. The snow thermodynamics is also
35 described in more detail, as requested by Reviewer 2. The motivation for the use of the
36 period 1980-1999 is also described more fully, also as requested by Reviewer 2.

37 No major corrections are present in the observational data description section.

1

2 **2.3 Sea ice state and surface radiation evaluation**

3 For this section, and all subsequent sections, the Arctic Ocean region has been refined to
4 exclude more of the Barents Sea, where processes are considered sufficiently different to
5 the rest of the Arctic Ocean as to render the assumptions used in the ISF analysis
6 questionable (for example there is high oceanic heat convergence here, and ice
7 concentrations are low or zero year-round). Figure 1, which maps this region, has been
8 changed accordingly.

9 In addition, unless stated otherwise, all model results are now given for the ensemble mean
10 of the 4 historical simulations of HadGEM2-ES (rather than for the first historical simulation
11 only, as had been the case for the previous version).

12 As a result of these changes, many of the sea ice thickness and surface radiation biases
13 quoted in Section 3 are different. The previous Figures 3-5 (presenting the evaluations) have
14 also been overhauled accordingly, and are now numbered Figures 2-4 (as discussed below,
15 it was decided that the previous Figure 2 was superfluous and has been removed).

16 The qualitative conclusions of the evaluation are unchanged: sea ice thickness is too low in
17 the annual mean and too amplified: net SW is too high and upwelling SW too low in the
18 summer, net LW and downwelling LW are too low in the winter.

19

20 **2.4 ISF method description**

21 This section has been completely rewritten, reflecting the changes in the methodology
22 described above. Firstly, the use of the word 'bias' is defined (as requested by Reviewer 2,
23 all instances of 'anomaly' the paper have been replaced with 'bias'). This is followed by a
24 discussion of the relationship between sea ice mass balance, surface flux and oceanic heat
25 convergence, clarified along the lines suggested by both reviewers, and with additional
26 evidence cited that in both HadGEM2-ES and in the real world, oceanic heat convergence is
27 a minor contributor to sea ice mass balance in the Arctic Ocean interior.

28 With the link between surface flux and sea ice mass balance established, the approach of
29 the study (see 2.1 above) is set out in detail. The formulae by which surface flux values are
30 estimated at each point in model space and time are described, and the assumptions behind
31 their derivation are discussed (as requested by Reviewer 1, Thorndike (1992) is cited at this
32 point, as it contains many of the key assumptions used).

33 Following the request by Reviewer 2 for a more detailed description of the method
34 application, the calculation of induced surface fluxes is then described in turn for three
35 climate variables (melt onset, downwelling LW and ice thickness), with the aid of a new
36 figure (Figure 5), which shows for each variable the fields of variable bias, surface flux
37 dependence, and induced surface flux bias. The calculation of the ice thickness component
38 is described in particular detail, as it now involves the estimation of thickness biases by
39 category which is nontrivial.

40 It is noted that in the updated analysis the treatment of the turbulent fluxes is changed; their
41 contribution is no longer neglected. However, they are treated in such a way that their

1 dependence on any climate variable examined cannot be evaluated, save for the ice area.
2 As a result of this change in emphasis, their omission is no longer justified in this section
3 (and the corresponding Figure 2 is removed); instead, the implications of their treatment is
4 discussed in the new Section 6.

5

6 **2.5 ISF results**

7 The presentation of the results of the ISF analysis has been changed in several ways.
8 Firstly, the ISF biases (with CERES as radiation reference dataset) are presented in the new
9 Table 1, following the request by Reviewer 1 for more systematic quantification of the
10 results. The table also shows total ISF bias, total net radiation bias relative to CERES, the
11 residual between the two, and the CERES-ERA1 net radiation bias, in preparation for a
12 discussion of the relationship between observational uncertainty and ISF uncertainty,
13 inspired by the request by Reviewer 2 for the ISF residuals to be discussed.

14 The results are also presented in Figure 6 (equivalent to Figure 6 in the previous version).
15 This figure is unchanged in essence, but now shows the ensemble mean induced surface
16 fluxes for the newly-refined Arctic Ocean region (see 2.3 above). Total ISF fluxes are also
17 shown more clearly, using black bars.

18 Following the presentation of Table 1 and Figure 6, the significant ISF biases are described
19 in turn (June surface melt onset, August ice area, early winter ice thickness, winter
20 downwelling LW). In each case, the bias is now quantified, and an equivalent figure for bias
21 in sea ice growth and melt is described, following the request by Reviewer 1 to make the
22 surface flux-sea ice mass balance link more explicit. Internal variability in the ISF biases is
23 then described, using all 80 ensemble years (Reviewer 2 request). Residuals between total
24 ISF and total net radiation biases are quantified and compared to observational uncertainty
25 in net radiation (Reviewer 2 request). The direct effect of observational uncertainty on ISF
26 biases is described. Potential errors in the ISF biases arising from method assumptions,
27 discussed in detail in Appendix A, are discussed (Reviewer 1&2 requests).

28 The discussion of ISF spatial patterns that follows has been left largely unchanged. A new
29 paragraph has been appended to this, comparing the spatial pattern in total ISF bias to that
30 in net radiation bias, with the aid of a new figure (Figure 7).

31

32 **2.6 Discussion**

33 Following the suggestion by Reviewer 1, the diagnosis of the thickness-growth and ice
34 albedo feedbacks from the ISF analysis has been justified in a new paragraph. The resulting
35 relative contributions (over the course of a year) of the feedbacks and forcings has been
36 quantified (both in terms of surface flux and sea ice melt/growth bias), thereby justifying a
37 statement in the abstract that Reviewer 1 had rightly questioned. The word 'forcing' has also
38 been defined more carefully, as it is different from the most commonly used meaning of this
39 word in a climate context.

40 Most of the ensuing discussion is unchanged, except for minor rewordings discussed in
41 Section 3 below, and a mention of Holland et al (2010), requested by Reviewer 2, at the
42 point at which it is concluded that the June surface albedo simulation problems are the

1 principal cause of of the low annual mean thickness of HadGEM2-ES. However, two
2 paragraphs have been appended, discussing the implications for the results of firstly the
3 imperfect treatment of turbulent fluxes, and secondly the omission of oceanic heat
4 convergence as an additional potential source of model bias in sea ice growth and melt. In
5 this second paragraph, HadGEM2-ES Arctic Ocean heat convergence is compared to
6 observational estimates, following requests by Reviewers 1&2.

7

8 **2.7 Conclusions**

9 This section has not undergone substantial changes as it is considered that the
10 methodological changes have not resulted in any changes to the conclusions of the study.
11 However, two paragraphs have been reworded for improved clarity.

12

13 **2.8 Appendix A (analysis of ISF errors)**

14 This section is equivalent to Appendix B in the original study, but is substantially larger and
15 is based on several suggestions by Reviewers 1&2 for ways in which errors in the ISF
16 analysis should be quantified. Its conclusions are quoted at the appropriate point in Section
17 5.

18 Firstly, the error in quantifying dependence of surface flux on climate variable is discussed.
19 This discussion is motivated by comparison of estimated surface flux fields to actual, as
20 suggested by Reviewer 2. As discussed above, although the new methodology has
21 improved the correspondence some differences remain, which can be categorised into three
22 types. In each case, a likely cause of the difference is stated, and its impact on the ISF
23 biases estimated.

24 Secondly, the error in characterising induced surface flux bias as a product of variable bias
25 with surface flux dependence is described. In this discussion, higher order derivatives of the
26 surface flux are evaluated. The error inherent in using the model state to evaluate surface
27 flux dependence is calculated using the mixed partial derivative terms (this follows from a
28 point made by Reviewer 2).

29

30 **3. List of minor corrections and rewordings**

31 In the following list, the page and line number references refer to the non-tracked changes
32 version of the manuscript. Each alteration is followed with an indication of whether it was
33 requested by Reviewer 1, 2 or neither (in the last case with additional justification).
34 Alterations which are directly related to the new structure, the new methods, or any of the
35 enhancements listed above, are not listed.

36 1-16 (abstract) 'Counteracting' removed (R2)

37 1-22 (Intro) '-' replaced with 'to' (R2)

38 1-27 Stammerjohn et al cited (R2)

39 1-28 'whoseloss' replaced with 'the loss of which' (R2)

- 1 1-34 'observations' replaced with 'reference datasets' (R2)
- 2 2-3 second 'very' removed (considered unnecessary)
- 3 2-15 'anomalies' replaced with 'biases' here and subsequently (R2)
- 4 4-4 (Model and observations) Reference to errors in atmospheric forcing added (R2)
- 5 4-14 'IceSAT' corrected to 'ICESat' and expanded
- 6 4-24 Unnecessary reference to ISCCP-D cloud product removed
- 7 4-28 'To the authors' knowledge' removed (considered irrelevant)
- 8 5-12 (Sea ice and surface radiation evaluation) 'Envisat' corrected to 'the ERS satellite
- 9 measurements' (this was previously incorrect)
- 10 15-1 (Discussion) Sentences reworded along the lines suggested in the original reviewer
- 11 response (R2)
- 12 15-20 'in the Arctic' added (for clarification)
- 13 17-14 (Conclusion) Paragraph reworded for clarity
- 14 17-19 Paragraph reworded for clarity
- 15 21-15 Acknowledgement expanded

16

17 **Appendix A: Original point-by-point reviewer response**

18

19 **A1. Reply to Reviewer Comment 1 (Anonymous)**

20 We thank the reviewer for taking the time to read our manuscript, and for his/her useful

21 suggestions for its improvement, which we address inline below. The reviewer's comments

22 are quoted in italics.

23

24 *West et al propose a new analysis framework to understand model biases in Arctic sea ice*

25 *which they apply to HadGEM2-ES, a model with known biases in sea ice characteristics.*

26 *The attribution of climate model errors in the sea ice zone is a very important open topic and*

27 *the paper provides original and likely efficient means to evaluate such errors. The main*

28 *problem I think is writing, which I found often imprecise, and renders a proper evaluation of*

29 *the paper difficult.*

30 *In particular, the methods absolutely require clarification and should use better and simpler*

31 *terminology. Because I did not fully get the methods, it was thereafter really complicated to*

32 *follow, in particular the discussion and conclusions.*

1 *A second requirement to make this paper acceptable is to early on in the result section to*
2 *explain that the induced surface flux method works - eg. to describe how well the different*
3 *methods to compute surface flux biases converge. Now this is done here and there, and I*
4 *have constantly been doubting of the quality of the methods, because of the absence of*
5 *such evaluation.*

6 The reviewer is right that the convergence of the different methods, demonstrated in Figure
7 6, deserves better discussion, and probably quantification, which we propose to carry out by
8 more thorough analysis of the errors of the induced surface flux method in Appendix B, and
9 discussion of these in Section 4, as described below.

10 Our view is that the spread amongst the different estimates is caused predominantly by
11 observational uncertainty, with errors introduced by the induced surface flux method
12 assumptions relatively small in magnitude by comparison. This is supported by the fact that
13 the difference between the sum of the induced surface flux contributions and each surface
14 flux anomaly is comparable in magnitude to the differences between surface flux anomalies
15 wrt the different datasets (ERA-Interim, ISCCP-FD, CERES).

16 We think that it would be difficult to show that the induced surface flux (ISF) method works
17 purely by comparison with the direct surface radiation evaluation, because the difference
18 between the different estimates are dominated by the observational uncertainty. We think a
19 better way would be by a more thorough evaluation of the impact of assumptions made by
20 the ISF method in Appendix B. For example:

- 21 • Evaluation of errors introduced by the simple model by comparing modelled fields of
22 net radiation to those predicted by the formulae, as suggested by Reviewer 2
- 23 • Evaluation of errors caused by ignoring higher-order derivatives, by calculating these
24 terms

25 The magnitude of these errors would then be compared to the observational uncertainty, as
26 estimated by the difference between the direct radiation evaluations shown in Figure 6.

27 There is a more fundamental point: the ISF method is not just a way of calculating surface
28 flux anomalies due to a particular process, but also of characterising them, because their
29 definition is to some degree subjective. For example, suppose for the month of May a model
30 shows mean downwelling SW of 300 Wm^{-2} , and albedo 0.8, given net SW of 60 Wm^{-2} , but
31 observational estimates shows mean downwelling SW of 250 Wm^{-2} , and albedo of 0.7,
32 giving net SW of 75 Wm^{-2} , with a model anomaly of 15 Wm^{-2} . Clearly the downwelling SW
33 anomaly induces a positive surface flux anomaly, the albedo anomaly induces a negative
34 one, and the total surface flux anomaly is -15 Wm^{-2} . But the exact induced anomalies are
35 subjective. The approach used in the paper is equivalent to multiplying the anomaly in one
36 process by the mean in the other, giving contributions of $+12.5 \text{ Wm}^{-2}$ and -27.5 Wm^{-2} by the
37 downwelling SW and albedo anomalies respectively.

38 Hence while it would in theory possible to say whether the *sum* of the ISF contributions was
39 correct (if we knew the exact actual surface flux error), it would not be possible to say
40 whether each individual contribution were correct. The main requirement is that each
41 contribution is physically realistic, and provides useful information.

42

1 *A third thing I would have enjoyed to see is a specific discussion of how the ice-albedo and*
2 *growth-thickness feedbacks can be diagnosed from the method. It is claimed in the abstract*
3 *that your method can separate these effects, and I am in trouble to see how that statement*
4 *is presently supported in the text. I can guess feedbacks are acting from Fig. 6, but I think*
5 *this topic deserves a bit more to support the claim made in the abstract.*

6 This does require greater justification. The sentence in which the relevant anomalies are
7 identified with the surface albedo feedback and thickness-growth feedback (page 10, line 31)
8 will be expanded accordingly.

9 The thickness-growth feedback, for example, ostensibly acts by altering the energy balance
10 at the base of the ice; as the ice thickens, the temperature gradient decreases, basal
11 conduction decreases, and the energy balance becomes less strongly negative, so the ice
12 thickens more slowly. But by energy conservation, this process must also have some
13 manifestation in the external fluxes: as the ice is losing energy less quickly, some external
14 energy flux must also have changed. Under the assumptions of the simple model used
15 (similar to Thorndike 1992 as you note below), which ignores sensible heat storage, it is the
16 upwelling LW term that changes: as the ice thickens, its top surface also cools to maintain
17 flux continuity.

18 Hence any change to the ice energy balance resulting from the ice thickening, and therefore
19 conducting less efficiently, can be diagnosed as the contribution of the ice thickness to the
20 change in upwelling LW radiation.

21

22 *I have also not understood why energetic errors of oceanic origin have been ignored from*
23 *the discussion, especially in the North Atlantic sector of the Arctic - where there is a low bias.*

24 Energy passing to the ice through the ocean-to-ice heat flux has two main sources: solar
25 input to the ocean, and oceanic heat convergence. The first is implicitly taken account of
26 through the analysis of the effect of ice fraction anomalies on net SW radiation. We make the
27 case that Arctic-wide, the importance of the oceanic heat convergence in driving summer
28 basal ice melt is small by comparison to direct solar input, and this will be more thoroughly
29 justified in the revision, referencing model results by e.g. Steele et al 2010 in addition to the
30 observational references originally included.

31 However, you are right that the contribution of the oceanic heat convergence should be
32 properly quantified. In the revised version of the paper, we will include estimates of Arctic-
33 wide ocean heat convergence (for model and observations), and set the results shown in
34 Figure 6 in this context.

35

36 *Finally, the authors claim in the conclusions that they can "quantify" the origin of errors, but*
37 *apart from Fig. 6 (which I liked a lot), I did not really see a quantification of the errors. Is*
38 *that quantification the main point - or is it the consistent comparison of the different sources*
39 *of error ?*

40 We do quantify individual contributions to the surface flux biases as shown in Figure 6 for a
41 few illustrative months, in section 4. However, we will examine whether there is scope for a

1 more systematic approach, for example quoting the annual average flux contribution for
2 each state variable in a table.

3

4 *Also, it was difficult to ultimately figure out whether biases in external forcings or in the sea
5 ice model are the ultimate cause of the biases. Is your method capable to tell after all ?*

6 Briefly, the answer is no: the method cannot tell the ultimate cause of the surface flux biases.
7 It is designed to diagnose the proximate cause of the biases.

8 The induced surface flux (ISF) method, alone, can determine only the first-order cause of the
9 net surface flux bias. The state variables examined (downwelling SW, downwelling LW, melt
10 onset occurrence, ice fraction, ice thickness) affect the surface flux on very short timescales,
11 and are unambiguously properties of the atmosphere (radiation) and sea ice (melt onset,
12 fraction, thickness). Hence the ISF method allows the short-term causes of surface flux bias
13 to be decomposed into those arising from the atmosphere, and from the sea ice.

14 It's recognised that the causes of biases in the state variables themselves may lie in different
15 systems. For example, ice thickness biases will have some ultimate cause in the
16 atmosphere – indeed, that is one finding of the paper. Conversely, while the case is made in
17 Section 5 that cloud errors are to blame for downwelling LW biases, it is likely that the sea
18 ice simulation will nevertheless have some influence on how this is manifested. However, all
19 these effects act on relatively long timescales, compared to the almost instantaneous
20 timescale on which the state variables affect the net surface flux.

21

22 *A last general comment - the logics of the arguments should be better presented.*

23 We apologise that the presentation of logic is unsatisfactory. This paper has been through
24 several rounds of restructuring as the analysis has developed, and the coherence of
25 argument has probably suffered due to this. We will try to significantly improve this in the
26 revision.

27

28 *I am pretty confident that - if these presentation issues are seriously addressed by the team
29 of coauthors, this will make an excellent contribution to their favourite cryospheric journal.*

30 *A few specific comments.*

31 —

32 ** I have tried to understand what the generic approach is. Here is what I have understood.
33 The present presentation is too lengthy, misses the essential elements and overdiscusses
34 details. A synthetic view is missing. There are three means to evaluate errors in surface
35 energy budget (I have understood two of them)*

36 *1) The direct computation of surface flux bias, i.e. the difference between simulated and
37 observed surface flux (or one of its components)*

1 This is correct although we would add the caveat that this is still only an estimate of the
2 actual surface flux bias – the observational uncertainty is very large.

3

4 *2) The induced surface flux bias, which is the contribution of bias in a specific variable to*
5 *surface flux bias, namely calculated as $\Delta F_x = dF_x / dx \Delta x(\text{mod-obs})$.*

6 *To evaluate derivatives, the SEB is simplified using two different approximations during the*
7 *cold and warm seasons, based on ideas from Thorndike et al 1992.*

8 *I don't think there is a need to calculate those derivatives in the body of the paper.*

9 We broadly agree but note the concern by Reviewer 2 that some of the calculations by which
10 the induced surface fluxes are arrived at are incompletely explained. It may be necessary to
11 show at least one derivative, for illustration, with the additional detail that is planned for the
12 revision.

13

14 *If the derivatives are well calculated and if the non-linearities are not too important, the sum*
15 *of ΔF_x should hopefully approach the surface flux bias.*

16 *3) The third diagnostic is "the sea ice latent heat flux uptake anomaly implied by the ice*
17 *volume anomalies relative to PIOMAS".*

18 *I have tried to figure out what the authors mean, but I did not really managed. The wording*
19 *is not precise enough for the reader to what is meant by this and what is gained by*
20 *comparing that to the surface flux biases. I guess "latent heat flux" is confusing in the*
21 *context of the surface energy budget. But whether that thing is a heat storage anomaly*
22 *divided by time or something else, I don't know. Maybe an "ice thickness bias converted to*
23 *Joules" or "an energetic equivalent ice thickness bias" ?*

24 This is correct. For each month, the modelled field of rate of change of ice thickness is
25 calculated as half the difference between the following and the preceding month. A similar
26 field is calculated for the reference dataset, PIOMAS. The reference field is subtracted from
27 the modelled field to create a model anomaly of ice thickness change. This is then multiplied
28 by ice density, specific latent heat of fusion, reversed in sign, and divided by the number of
29 seconds in a month, to create an equivalent sea ice latent heat storage anomaly in Wm^{-2} .

30 For the reasons discussed in Section 2.3, the surface heat flux is viewed as the main source
31 of this latent heat storage. It's noted however that it would be useful to provide an estimate
32 of modelled and observed oceanic heat convergence which provides an additional input to
33 the latent heat storage.

34 We will clarify this point in the revised manuscript.

35

36 *Besides an explanation of what it means, we would need an explanation of what should be*
37 *taken from that diagnostic.*

1 *It is important to clarify this point because a lot of the argumentation was based on that.*

2 * *The two methods to compute the surface flux derivatives is called "a model". I think it is a*
3 *"computation method". It is actually inspired from Thorndike et al (1992) – which should be*
4 *acknowledged - and maybe from earlier works in EBMs. What you are doing is to derive the*
5 *surface energy budget wrt anything.*

6 The 'model' versus 'computation method' is an interesting distinction – our interpretation is
7 that it hinges on whether the formulae are viewed as a way of calculating induced surface
8 fluxes (model) or characterising them (computation method), as discussed above. As in our
9 view both are valid interpretations, either phrase might be more appropriate depending on
10 the circumstances.

11 Thorndike et al will be cited.

12

13

14

15 **A2. Reply to reviewer comment 2 (Francois Massonnet)**

16 We thank Francois Massonnet for his helpful and thorough review of our manuscript. Below,
17 we address in turn his major and minor comments inline, which are quoted in italics.

18

19 **Major comments**

20 1) *It is not always easy to follow the authors' methodology. I see the general idea behind*
21 *the approach: expressing the net flux to the ice as a function of state variables, then*
22 *linearizing around a reference state to obtain the flux bias resulting from the bias in*
23 *one of the model components. However, I could surely not reproduce the results*
24 *myself, just based on the text. I appreciate the efforts to publish the code in*
25 *Supplementary Material, but the text itself should have all elements. For example, I do*
26 *not understand how the bias in F_{sfc} attributed to error in melt onset is derived (i.e.,*
27 *from eq. A6 to 4). Furthermore, the attribution of flux error to melt onset error*
28 *seems to not be a function of the melt onset itself, but rather a function of*
29 *concentration difference. This is confusing: melt onset is defined by the time of the*
30 *day where surface melting commences, and the right hand side of Eq. 4 does not*
31 *display surface melting terms. At some point it came to my mind that the authors were*
32 *perhaps using "melt onset" for "ice retreat", but I'm not sure. In all cases, this is*
33 *confusing.*

34 The definition of the state variable 'melt onset occurrence', and its relation to the net surface
35 flux, is not very clearly explained in the paper, and certainly requires expansion. This will be
36 altered in the revised version of the paper, and we will ensure more generally the replicability
37 of the calculations of the induced surface fluxes (for example, noting the use of local ice and
38 snow thicknesses as you suggest below). However, a brief explanation of this particular
39 component, melt onset occurrence, is also provided here. Very simply, its purpose is to
40 capture the effect of meltpond formation on the surface flux.

1 HadGEM2-ES parameterises the effect of meltponds by reducing surface albedo linearly
2 from 0.8 to 0.65 as the surface temperature goes from -1°C to 0°C, after Curry et al (2001).
3 Because we have daily surface temperature fields, we can judge for each modelled year
4 which day 'melt onset' – defined as the day surface temperature first goes above -0.5°C –
5 occurs. Comparison of these dates to the observational SSMI estimates referenced in the
6 paper shows that modelled melt onset occurs, on average, 20-25 days earlier across most of
7 the Arctic Ocean in the model than in observations.

8 In the induced surface flux analysis, we examine the effect on modelled surface flux of the
9 melt onset process occurring at the wrong time of year. The relevant state variable here is
10 'melt onset occurrence', which takes the value 0 or 1 depending on whether a grid cell on a
11 particular day has yet exceeded -0.5°C (model definition) or whether a liquid water
12 microwave signature has been detected (observational definition). In a similar way to the
13 other state variables used in the paper, the observations are averaged over the period 1980-
14 1999 to obtain a daily climatology of melt onset occurrence. For each modelled year, this
15 climatology is subtracted from the modelled melt onset occurrence fields to obtain a
16 modelled melt onset anomaly. This anomaly is then multiplied by the relevant partial
17 derivative – in this case, (downwelling SW) * (cold snow albedo – melting snow albedo) to
18 produce the induced anomaly in net SW.

19

20 2) *Besides the need for clarity in the methodology, a key question is to what extent the*
21 *assumption of linearity holds, in particular for what bias range Eqs 3 and 4 would be*
22 *valid. Will the methods work for models with very large biases? Another point is that*
23 *this linearization involves the use of Eqs 1 and 2, that are themselves derived using*
24 *linearity assumptions. I trust that the approach is valid, because the sum of*
25 *individual contributions (Fig. 6) seems to match the flux errors from datasets*
26 *and from volume estimates, but a quantification of this match should be done*
27 *(perhaps by calculating residuals). Overall I find that the authors have not discussed*
28 *the validity of this assumption, and this is critical given how non linearly the ice*
29 *behaves.*

30 You are right that this needs to be quantified. For some of the state variables the
31 dependence of surface flux is linear, and the second partial derivatives go to zero (e.g. all
32 state variables in the melting season, and downwelling LW in the freezing season). However
33 the dependence of surface flux on ice and snow thickness is nonlinear and it would be useful
34 to examine the circumstances in which higher derivatives are important.

35 As you mention, additional assumptions are made in deriving equation (1): linearity of
36 upwelling longwave dependence on surface temperature, and uniform conduction of heat
37 within the ice. We will try to quantify the impact of these also by comparing actual net
38 surface flux fields to predicted fields, as you suggest below in point 5).

39

40 3) *I would also like to see if the method is robust to internal variability. Could the authors*
41 *take one or several of the four other members of the HadGEM2-ES model and run the*
42 *same analysis? In other words, is the 1980-1999 period long enough to identify and*
43 *attribute the biases?*

1 Analysis of other ensemble members would be a valuable enhancement of the study. For
2 the revised version of the paper, we plan to carry out the same analysis on the other three
3 ensemble members, and to quantify the consistency with the results from the first member.

4

5 4) *The authors have not cited an important study: Holland et al., 2008*
6 *(doi:10.1007/s00382-008-0493-4). In that study, the inter-model scatter in the sea ice*
7 *mass budget (present-day conditions) is shown to be explained by the way models*
8 *absorb shortwave radiation. This is directly relevant to the study here, and I think the*
9 *authors should go through the Holland et al. study to position their results with respect*
10 *to theirs. In particular the claim that turbulent fluxes are of relatively minor importance*
11 *relative to radiative fluxes in setting the surface energy balance (Fig. 2, and p. 5 line*
12 *11-16) should be put in perspective with that study. As the Arctic sea ice mean state*
13 *changes, turbulent fluxes appear to be of increasing importance.*

14 Holland et al (2008) show annual sea ice melt rates to be strongly correlated with summer
15 net SW across the CMIP3 ensemble. The causality here could go in either, or most likely
16 both, directions. This appears to be consistent with the finding in the current study that the
17 excessive sea ice melt in HadGEM2-ES is driven by surface albedo and net SW issues. This
18 will be referenced.

19 The neglecting of turbulent fluxes is a shortcoming of our study. As you point out, while they
20 are comparatively small in an absolute sense, they may nevertheless be important in driving
21 future changes. In a similar way, model anomalies in turbulent fluxes may be of comparable
22 size to those in radiative fluxes even if the model absolute values are much smaller. We will
23 expand on this point in the Discussion.

24

25 5) *The authors should prove, with a figure, that the model developed in the appendix is*
26 *good enough to do the investigations. Could they plot, for one or several grid cells and*
27 *one or several freezing seasons, the reconstructed flux F_{sfc} (Eq. A4) and the actual*
28 *flux from the model? A quantification of the correspondence would be a plus.*

29 This would also be a valuable exercise. Actual and calculated modelled fields will be
30 compared for a few sample years, and the correspondence described, quantified and
31 illustrated. The most appropriate place for this would probably be the discussion of errors in
32 Appendix B.

33

34 6) *Nothing is said about the treatment of snow in the HadGEM2-ES model. How many*
35 *snow layers are there, what is snow conductivity, etc.?*

36 There is only one snow layer, and the conductivity is $0.33 \text{ Wm}^{-1}\text{K}^{-1}$. Like the ice, the snow
37 has no heat capacity. It should be made clear, however (here and in the revised version of
38 the paper) that sensible heat storage is parameterised in the top 10cm of the snow-ice
39 column during surface exchange calculations, to aid stability.

40

1 7) *The authors repeatedly use the word "anomaly" to describe the difference between*
2 *modeled and reference quantities, but I would avoid this word and use "bias" or*
3 *"error" instead. To me, an "anomaly" is used to describe the deviation of a signal*
4 *with respect to its own mean*

5 We have some concern is that use of the word 'bias' might suggest that HadGEM2-ES is
6 being evaluated with respect to the 'truth', but most datasets used are only very rough
7 approximations to this. We will change 'anomaly' to 'bias', but clearly define at the outset the
8 meaning of the word 'bias' for the purposes of the paper – the difference of the model
9 relative to a particular observational estimate.

10

11 8) *I'm unclear about whether ocean surface temperature biases are accounted for in the*
12 *analysis. From Fig. 6, it looks like they are not. On the other hand, p. 5 lines 6-10*
13 *seem to suggest that the Arctic Ocean is critical in setting the ice energetic balance*
14 *(and this is also seen in Keen et al ([https://link.springer.com/article/10.1007/s00382-](https://link.springer.com/article/10.1007/s00382-013-1679-y)*
15 *013-1679-y*, their Fig. 4). *So, I'm puzzled: is the contribution of oceanic surface*
16 *temperature bias taken into account or not in the analysis?*

17 It is true that the ocean contributes a significant amount of heat to the ice in the summer.
18 However, we make the case in our study that the major part of this heat comes from direct
19 solar heating of the ocean, an effect which is taken account of through analysis of the effect
20 of ice fraction on the net SW bias. This case will be strengthened in the revision by citing
21 evidence from models (e.g. Steele et al, 2010) in addition to the evidence from observations
22 already referenced.

23 This is also relevant to the minor comment at 5-6/10 below.

24

25

26 **Minor comments**

27 1-18 - *"countered by a counteracting" is a bit odd.*

28 'Counteracting' is superfluous and will be removed.

29

30 1-24 - *"from 1986-2015" -> from 1986 to 2015*

31 Change will be made as suggested.

32

33 1-28 - *Along with an earlier melt onset date, you can mention that freeze up has*
34 *been delayed: Stammerjohn et al., 2012, their Fig.2 (doi:10.1029/2012GL050874)*

35 This will be done.

36

37 1-29 - *"whoseloss" -> "the loss of which"*

1 Change will be made as suggested.

2

3 *2-1 - Evaluation against observations of volume is quite impossible (even extent*
4 *observations are not direct observations), so I would use "observational or reanalysis*
5 *reference datasets"*

6 Change will be made as suggested.

7

8 *2-18 Instead of "anomalies" I would use "biases"*

9 See response to point 7) above.

10

11 *3-24 The period 1980-1999 is used for evaluation, because it "predates the rapid sea ice*
12 *loss". Why is it a problem to have a period with strong trend in the analysis? Is it expecting*
13 *that the SEB would change too rapidly during a period with strong trends? Would the*
14 *analysis be robust if the model output was evaluated on a distinct and later period (2000-*
15 *2015 for instance, using historical + RCP8.5 runs). Please elaborate.*

16 The trend itself is not problematic. Our motivation for using this period was to evaluate the
17 model on a 'reference' time period at least partially independent of the time period that is
18 usually used to evaluate sea ice trends. We will make this clear in the revised version.

19

20 *3-35 Reanalysis data also suffer from biases because of errors in atmospheric forcing, this*
21 *could be stated as well.*

22 This will be stated.

23

24 *5-11/16 Can the authors explain exactly what they mean by "Heat flux due to snowfall". The*
25 *presence of snow affects heat conduction fluxes and acts to reduce bottom growth, is that*
26 *what the authors are talking about?*

27 The presence of snow matters only because it takes energy to melt it; snow falling on ice
28 changes the enthalpy of the snow-ice system. A 3m column of bare fresh ice at 0°C, for
29 example, will take $\sim 9.2 \times 10^8 \text{ Jm}^{-2}$ to melt it. If 50cm fresh snow falls on the ice, the
30 combined snow-ice column will take $\sim 9.8 \times 10^8 \text{ Jm}^{-2}$ to melt it. Hence the falling of snow on
31 ice represents a transfer of negative latent heat from the atmosphere system to the snow-ice
32 system, which must be taken account of in calculating the total surface flux. We will try to
33 explain this more fully in the revised version of the paper.

34

1 5-26 I assume h_l and h_s refer to in-situ / actual thickness (this is the one that matters
2 for vertical thermodynamics). It would be good to mention that here, as there is usually a
3 lot of confusion between that quantity and the grid cell average thickness.

4 Yes, this is the case and that will be clarified.

5

6 5-24 Eq. 1: Maybe I missed it, but what is the value for ice albedo? Does albedo depend
7 on the ice state?

8 The ice albedo used is 0.61. This does not depend on ice thickness, but falls linearly to
9 0.535 as ice surface temperature rises from -1°C to 0°C . This information will be added to
10 the text.

11

12 5-27 The subscript for snow thickness is "S" here while it is "s" elsewhere

13 Change will be made as suggested.

14

15 5-28 The symbol for albedo is α_l while in the equation it's α_{ice}

16 Change will be made as suggested.

17

18 5-30 Eq. 2: the big "dot" is a bit disturbing, it makes me think at a scalar product. I would
19 use a simple dot or no dot at all.

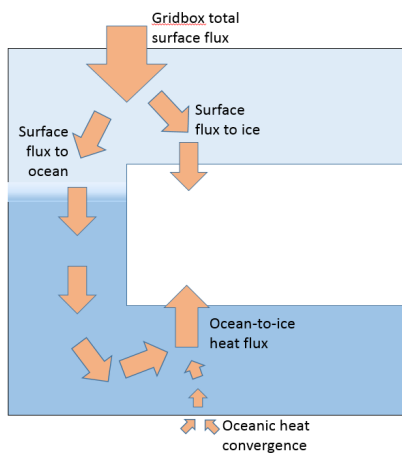
20 Change will be made as suggested.

21

22 5-6/10 The sentence "Because of this, although advection-derived ocean heating..." is
23 unclear to me. First, can you demonstrate the oceanic heat convergence (that is not
24 accounted for in your framework) is a small contributor to volume changes? Second, I do not
25 follow the logical articulation with the next sentence "Hence the surface energy...". Please
26 clarify. In the same line, reading the recent paper by Lei et al. (2018,
27 doi:10.1002/2017JC013548) could be useful to add up to the discussion.

28 Regarding your first question, Reviewer 1 also suggested that it would be sensible for the
29 oceanic heat convergence to be properly quantified, and this will be done in the revised
30 version.

31 Regarding your second question, see first our response to your major comment 8) above.
32 We agree our wording here is confusing. The case we are making is probably best illustrated
33 by this schematic:



1

2 The point made is that the source energy for the ocean-to-ice heat flux derives, in the main,
 3 from the surface heat flux (specifically, solar heating in summer), and not from oceanic heat
 4 convergence, over most parts of the Arctic Ocean (clearly there are regions where this is not
 5 true, e.g. near the ice edge in the Atlantic sector). Therefore the surface flux analysis
 6 (specifically, the effect of ice fraction anomalies on net SW) implicitly accounts for a large
 7 part of the ocean-to-ice heat flux.

8 As we mention above, additional evidence will be cited for this in the revision, as well as
 9 rewording this sentence.

10 Thank you for drawing our attention to Lei et al (2018), which draws together a very wide
 11 range of observational data to investigate mechanisms of sea ice growth and melt. If we
 12 have understood this study correctly, it deduces a strong role for direct solar heating in
 13 driving summer sea ice basal melting by noting an association between areas of low
 14 summer sea ice concentration and high early autumn oceanic heat fluxes (as measured by
 15 ice mass balance buoys). Hence this would also be a valuable study to quote in this context.

16

17 *6-1 Please give the albedo values used.*

18 These will be provided in the revised version: 0.535 for melting ice, 0.61 for cold ice, 0.65 for
 19 melting snow, 0.8 for cold snow.

20

21 *6-3 "summarises" -> "summarise"*

22 Change will be made as suggested.

23

24 *6-10 Eq.3: please describe the meaning of the terms of the equation. In particular, what is*
 25 *h_{l_eff} ?* It is necessary to have this information in the text somewhere.

26 These will be described fully.

1

2 *6-23 The partial derivatives are to be evaluated at a reference state, and I understand here*
3 *that a mid-point between observations and model is taken ("Where observational datasets*
4 *were available, the reference quantities in the partial derivative fields were calculated as*
5 *model-observation means"). The authors should explain why it was done this way. I assume*
6 *that the reconstructed flux error would be mathematically closer to the actual error than if the*
7 *reference was taken as either the model or the osbserved value.*

8 I don't think that's the case. For any function f , evaluated at two values x_1 and x_2 , if we try to
9 approximate $f(x_2)-f(x_1)$ using the first term of the Taylor series evaluated at some point λx_1
10 $+(1-\lambda)x_2$, where $0 \leq \lambda \leq 1$, the coefficient of the second Taylor series term is minimised when
11 $\lambda=1/2$, i.e. at the midpoint of x_1 and x_2 . Hence evaluating the partial derivatives at the model-
12 observation midpoint provides our best guess. We will briefly note our reasoning for using
13 this in the revision.

14

15 *6-30 The paragraph starts by saying that 4 ensemble members were run, but Fig. 3 only*
16 *shows one. Can you clarify?*

17 Only one ensemble member is used for the analysis – this will be clarified, although as
18 indicated above reference will be made in the revised version to results for the other three
19 members.

20

21 *8-28 The word "save" should be removed, I think*

22 It would probably be best replaced by 'except for'.

23

24 *10-25/28 Can you go a bit more quantitative here? From Fig. 6, the residual of the analysis*
25 *can be calculated as the sum of individual contributions (the stars) and the actual flux error.*

26 But what is the 'actual flux error'? The surface flux anomalies wrt ERAI, ISCCP-FD, CERES
27 cannot be regarded as such because of the observational uncertainties – this is clear,
28 because the difference between the sum of the contributions and each surface flux anomaly
29 is comparable in magnitude to the differences between surface flux anomalies wrt the
30 different datasets. Each is only an estimate of the actual flux error, which cannot be exactly
31 known – it is equally possible that the sum of the contributions is a more accurate estimate
32 than any.

33 We can provide the residual of the analysis for completion with respect to ERAI, ISCCP-FD
34 or CERES – but the actual numbers will differ greatly depending on which dataset is used.

35

36 *10-31/32 The surface albedo feedback is not just a sea ice concentration thing. The melting*
37 *of snow, the thinning of the ice are also key players in the surface albedo reduction, even*

1 *though ice concentration remains unchanged. Wouldn't it make more sense to include these*
2 *factors as well in the definition of surface albedo feedback?*

3 It is true that the surface albedo feedback also includes these effects. However, it would not
4 be possible to include the effect of snow melting because of the lack of reference dataset.
5 The effect of ice thickness on albedo is not actually modelled by HadGEM2-ES – the albedo
6 switches abruptly to the open ocean value when the sea ice thickness falls to zero. Hence
7 there would be two separate effects to estimate here: the direct effect of ice thickness
8 anomalies on albedo, and the effect of HadGEM2-ES not modelling this. Given this, as well
9 as large uncertainties in observations of the link between albedo and ice thickness for thin
10 ice, we think this effect is outside the scope of the study. However, it will be mentioned as a
11 possible additional contributing factor to the summer net SW bias.

12

13 *11-15 The sentence "Hence the melt onset anomaly, acting alone, would induce a seasonal*
14 *cycle of sea ice thickness both lower, and more amplified, than that observed..." is unclear,*
15 *especially regarding the "lower" part. Can you please rephrase?*

16 How would the following be:

17 'Hence the melt onset anomaly, acting alone, would induce a seasonal cycle of sea ice
18 thickness lower in the annual mean, but also more amplified, than that observed, because
19 the surface albedo and thickness-growth feedbacks act to translate lower ice thicknesses
20 into faster melt and growth. For similar reasons, the downwelling LW anomaly, acting alone,
21 would induce a seasonal cycle of sea ice thickness higher in the annual mean, and also less
22 amplified, than that observed.'

23

24 *12-1 "concludethat" -> conclude that*

25 Change will be made as suggested.

26

27 *Fig. 3. I'm puzzled by panel (a). Sea ice extent seems small. Is that because the domain*
28 *"Arctic Ocean" is restricted to the seas of Fig. 1? In other observational records, like NSIDC,*
29 *winter sea ice extent is more in the 14-16 million km² range.*

30 Yes, the extent is calculated over only the Arctic Ocean domain, like other variables in this
31 paper, and so the winter extent appears much lower than in the well-known NSIDC figures.
32 We think that this is appropriate, because much of the winter variability in whole-Arctic sea
33 ice extent is due to processes in the subpolar seas, which are not relevant to the Arctic
34 Ocean process analysis in this study.

35

36

37 **References**

1 Steele, M.; Zhang, J.; Ermold, W. (2010): Mechanisms of summer Arctic Ocean warming, J.
2 Geophys. Res. (Oceans), 115, C11, doi: 10.1029/2009JC005849

3

4 **Appendix B: Tracked changes version of document**

5

6

7

8

9

10

11

12 **Attribution of sea ice model biases to specific model errors** 13 **enabled by new induced surface flux framework**

14 Alex West¹, Mat Collins², Ed Blockley¹, Jeff Ridley¹, Alejandro Bodas-Salcedo¹

15 ¹Met Office Hadley Centre, FitzRoy Road, Exeter, EX1 3PB

16 ²Centre for Engineering, Mathematics and Physical Sciences, University of Exeter, Exeter, EX4 4SB, UK

17 *Correspondence to:* Alex E. West (alex.west@metoffice.gov.uk)

18 **Abstract.** A new framework is presented for analysing the proximate causes of model sea ice biases,
19 demonstrated with the CMIP5 model HadGEM2-ES. ~~Arctic sea ice extent has decreased over recent decades~~
20 ~~and has reached historic minima in late summer in recent years. Climate models project an ice-free Arctic in late~~
21 ~~summer during the 21st century, with wide-ranging implications for global climate and geopolitics. However,~~
22 ~~substantial spread remains in climate model projections of the rate of sea ice decline, with drivers poorly~~
23 ~~understood. In the framework described, In this framework~~ the sea ice volume is treated as a consequence of the
24 integrated surface energy balance. A system of simple models allows the local dependence of the surface flux,
25 as a function of time and space, on specific model variables (ice area, ice thickness, surface melt onset and
26 downwelling longwave and shortwave radiation) to be described. When these are combined with reference
27 datasets of the variable in question, it is possible to estimate the surface flux bias induced by the model bias in
28 that variable. ~~specific portions of the surface flux anomaly to be attributed to individual processes by calculating~~
29 ~~for each process an 'induced surface flux anomaly'~~. The method allows ~~detailed~~ quantification of the role played
30 by the surface albedo and ice thickness-growth feedbacks in causing anomalous sea ice melt and growth to the
31 role played by other forcings which can be viewed as external to the sea ice state on short timescales. It shows
32 biases in the HadGEM2-ES sea ice volume simulation to be due to a bias in spring surface melt onset date,
33 partly countered by a ~~counteracting~~ bias in winter downwelling longwave radiation. The framework is

1 applicable in principle to any model and has the potential to greatly improve understanding of the reasons for
2 ensemble spread in modelled sea ice state.

3

4 **1. Introduction**

5 The Arctic sea ice cover has witnessed rapid change during the past 30 years, most notably with a decline in
6 September extent of $1.05 \times 10^6 \text{ km}^2$ / decade from 1986 ~~to~~-2015 (HadISST1.2, Rayner et al 2003). In
7 association with the changes in extent, evidence of declining Arctic sea ice thickness has been observed from
8 submarine and satellite data (Rothrock et al, 2008, Lindsay and Schweiger, 2015). Arctic sea ice is also thought
9 to have become younger on average as reserves of older ice have been lost (Maslanik et al, 2011), ~~and~~the
10 ~~beginning-onset~~ of summer melt-~~onset~~ has been observed to become earlier in the year (Markus et al, 2009) ~~and~~
11 ~~the onset of winter freezing has been observed to become later (Stammerjohn et al, 2012).~~

12 The changes have focussed much interest on model projections of Arctic sea ice, ~~whose loss the loss of which~~
13 influences the climate directly through increased absorption of shortwave (SW) radiation during summer and
14 through greater release of heat from the ocean to the atmosphere during winter (Stroeve et al, 2012b). However,
15 substantial spread remains in model simulations of present-day Arctic sea ice, and of the long-term rate of
16 decline under climate change (Stroeve et al, 2012a). The causes of this spread are at present poorly understood,
17 resulting in considerable uncertainty in future projections of Arctic sea ice.

18 Evaluating sea ice extent or volume with respect to ~~observations-reference datasets~~ shows that some models
19 clearly reproduce present-day sea ice state more accurately than others (e.g. Wang and Overland, 2012;
20 Massonet et al, 2012; Shu et al, 2015). However, an accurate simulation of sea ice extent and volume under the
21 present-day climate does not necessarily imply an accurate future projection of sea ice change, as a correct
22 simulation can be obtained by accident due to cancelling model errors, or internal variability. Sea ice extent in
23 particular is known to be a very unsuitable metric for diagnosing model performance due to its ~~very~~-high
24 internal variability (Notz, 2015; Swart et al, 2015). Hence there is a need to better understand the drivers which
25 lead a model to simulate a given Arctic sea ice state.

26 Ice volume is, to first order, proportional to the heat required to melt the ice, and therefore acts to integrate the
27 surface and basal energy balance. Basal melting in the interior ice pack has been shown to derive in the main
28 from direct solar heating of the ocean (e.g Maykut and McPhee, 1995), while basal freezing derives principally
29 from conduction of energy upward through the ice (Perovich and Elder, 2002); this implies that the surface
30 energy balance (SEB) contains the principal sources and sinks of energy for the sea ice on an Arctic-wide scale.
31 However, a complex two-way relationship exists between sea ice thickness and surface energy balance, via the
32 surface temperature and surface albedo, giving rise to the thickness-growth feedback (Bitz and Roe, 2004) and
33 the surface albedo feedback (Bitz, 2008), both of which exert first-order control on the sea ice state. Hence
34 many components of the SEB cannot be viewed as independent of the sea ice state in any meaningful sense.

35 This study, which presents a new framework to investigate the causes of modelled sea ice ~~biases anomalies~~, is
36 motivated by a desire to separate, to first order, many external drivers of the SEB (and hence the sea ice state)
37 from the thickness-growth and albedo feedbacks, and thereby ~~better~~ understand the processes that result in a

1 particular modelled sea ice state being simulated. The analysis uses as a case study the four members of the
2 historical ensemble of the coupled model HadGEM2-ES, a member of the CMIP5 historical ensemble
3 model which simulates anomalously low annual minimum ice extent, and which simulates an ice volume which
4 is both too low in the annual mean and too amplified in the seasonal cycle, a similar behaviour to that identified
5 by Shu et al (2015) in the CMIP5 ensemble mean.

6 In the framework presented, the total surface flux~~principal components of the SEB, shortwave and longwave~~
7 radiative fluxes, are is expressed in terms of key Arctic climate variables as functions of space and time using
8 two simple models, for the freezing and melting seasons respectively, which are shown to capture well the large-
9 scale spatial and seasonal variation of the surface flux. With the use of the simple models, the local dependence
10 of modelled surface flux on key variables can be described. Hence, using~~and~~ reference datasets for the climate
11 variables, the model bias~~anomaly~~-in surface flux induced by each climate variable can be estimated. In this
12 way, biases ~~anomalies~~-in ice growth and melt over the course of the year are attributed via the SEB~~surface flux~~
13 to biases in specific model quantities. The method allows the contributions to model biases ~~anomalies~~-in ice
14 growth and melt caused by~~of~~ the sea ice albedo feedback, the ice thickness-growth feedback, and ~~of~~-various
15 external factors, to be separately quantified. In this way it can be seen how model biases in the external drivers
16 are able to produce a particular sea ice state, offering a valuable tool for setting sea ice state biases in context,
17 and for understanding spread in sea ice simulation within multimodel ensembles.

18 In Section 2, the HadGEM2-ES model and the observational datasets used are described in turn, ~~and the induced~~
19 ~~surface flux method is introduced~~. In Section 3 the sea ice and surface radiation simulations of HadGEM2-ES
20 are evaluated. In Section 4, the induced surface flux method is introduced, and ~~in~~ Section 5~~4~~ the induced
21 surface flux analysis is applied to HadGEM2-ES, allowing quantification of the role played by biases ~~anomalies~~
22 in specific Arctic climate variables in causing anomalous ice growth and melt. In Section 6~~5~~ the implications of
23 the results are discussed, in particular the mechanisms by which the identified external drivers identified ~~cause~~
24 determine the modelled sea ice state, and the likely drivers behind the corresponding model biases. Conclusions
25 are presented in Section 7~~6~~.

26

27 **2. Model and observational d~~Data and methods~~**

28 **2.1 The HadGEM2-ES model**

29 HadGEM2-ES is a coupled climate model employing additional components to simulate terrestrial and oceanic
30 ecosystems, and tropospheric chemistry (Collins et al, 2011). It is part of the 'HadGEM2' family, a collection of
31 models that all use the HadGEM2-AO coupled atmosphere-ocean system. HadGEM2-AO is developed from
32 HadGEM1 (Johns et al, 2006), a coupled atmosphere-ocean model whose sea ice extent simulation was
33 recognised as being among the closest to observations out of the CMIP3 ensemble models (Wang and Overland,
34 2009). While the atmospheric and ocean components of HadGEM2-ES contain a large number of improvements
35 relative to HadGEM1, many of these targeted at improving simulations of tropical weather, the sea ice
36 component is very similar to that of HadGEM1 except for three minor modifications (Martin et al, 2011, table
37 A4).

1 | A fundamental feature of the sea ice component of HadGEM2-ES, which is important for the analysis
2 | described in Section 4 below, is that it includes a sub gridscale sea ice thickness distribution (Thorndike et al,
3 | 1975). In this formulation, ice in each grid cell is separated into five thickness categories with boundaries at 0,
4 | 0.6m, 1.4m, 2.4m, 3.6m and 20m, each with its own area, thermodynamics and surface exchange calculations.;
5 | It also includes elastic-viscous-plastic sea ice dynamics (Hunke and Dukowicz, 1997) and incremental
6 | remapping (Lipscomb and Hunke, 2004). The thermodynamic component is a zero-layer model, with no heat
7 | capacity, described in the appendix of Semtner (1976). The insulating effect of snow is modelled by means of a
8 | single layer with conductivity 0.33Wm⁻¹K⁻¹, also with no heat capacity (although sensible heat storage is
9 | parameterised in the top 10cm of the snow-ice column during surface exchange calculations, to aid stability).
10 | Most processes are calculated in the ocean model, but the SEB surface energy balance (SEB) calculations are
11 | carried out in the atmosphere model, which passes top melting flux and conductive heat flux to the ocean model
12 | as forcing for the remaining components. A more complete description of the is sea ice component can be found
13 | in McLaren et al (2006).

14 | This study uses the first four ensemble members of the CMIP5 'historical' experiment of HadGEM2-ES, forced
15 | with observed solar, volcanic and anthropogenic forcing from 1860 to 2005. The period 1980-1999 is chosen for
16 | the model evaluation, as a period which predates much of the recent rapid Arctic sea ice loss, and is hence at
17 | least partially independent of the period normally used to evaluate sea ice trends. It has the added advantage of
18 | being with its associated climatic changes, and which is recent enough to allow the use of a reasonable range of
19 | observational data. All analysis is carried out with data restricted to the Arctic Ocean region, shown in Figure 1.

20

21 | 2.2 Observational data

22 | Uncertainty in observed variables tends to be higher in the Arctic than in many other parts of the world. There
23 | are severe practical difficulties with collecting in situ data on a large scale over regions of ice-covered ocean.
24 | While satellites have in many cases been able to produce Arctic-wide measurements of some characteristics,
25 | most notably sea ice concentration, the relative lack of in situ observations against which these can be calibrated
26 | means knowledge of the observational biases is limited. Reanalysis data over the Arctic is also more subject to
27 | the reanalysis model errors than in other regions, due to errors in atmospheric forcing, and the existence of as
28 | there are fewer direct observations available for assimilation (Lindsay et al, 2014). The approach of this study is
29 | to use a wide range of observational data to evaluate modelled sea ice state and surface radiative fluxes, and to
30 | use as reference datasets for the induced surface flux framework, using the small number of in situ validation
31 | studies to set results in context as far as possible.

32 | To evaluate modelled sea ice fraction, we use the HadISST1.2 dataset (Rayner et al, 2003), derived from passive
33 | microwave observations. To evaluate modelled sea ice thickness Arctic-wide, we use the ice-ocean model
34 | PIOMAS (Schweiger et al, 2011), which is forced with the NCEP reanalysis and assimilates ice concentration
35 | data. Laxon et al (2013) and Wang et al (2016) found PIOMAS to estimate anomalously low winter ice
36 | thicknesses compared to satellite observations in some years. In particular, Wang et al (2016) found PIOMAS to
37 | have a mean bias of -0.31m relative to observations from the Ice, Cloud and land Elevation
38 | Satellite satellite-laser sensor. To set the PIOMAS comparison in context, we use two additional datasets to

1 evaluate the model over smaller regions; measurements from radar altimetry aboard the ERS satellites from
2 1993-2000 (Laxon et al, 2003), limited to latitudes below 82°N; and estimates compiled by Rothrock et al
3 (2008), derived from a multiple regression of submarine transects over the Central Arctic Ocean from 1975-
4 2000, constrained to be seasonally symmetric.

5 To evaluate modelled surface radiative fluxes across the whole Arctic Ocean, three datasets are used. Firstly, we
6 use the CERES-EBAF (Clouds and Earth's Radiant Energy Systems – Energy Balanced And Filled) Ed2.7
7 dataset (Loeb et al, 2009), based on direct measurements of top-of-atmosphere radiances from EOS sensors
8 aboard NASA satellites, available from 2000 – present. Secondly, we use the ISCCP-FD (International Satellite
9 Cloud Climatology Project FD-series) product, ~~derived from the ISCCP-D cloud product described below using~~
10 ~~a radiative transfer algorithm~~ (Zhang et al, 2004). Lastly, we use the ERA-Interim (ERA-Interim) atmospheric
11 reanalysis dataset, which provides gridded surface flux data from 1979-present using a reanalysis system driven
12 by the ECMWF (European Centre for Medium-range Weather Forecasts) IFS forecast model and the 4D-Var
13 ~~atmospheric~~-data assimilation system (Dee et al, 2011).

14 ~~[To the authors' knowledge, in-situ validation of these datasets in the Arctic has been quite limited, but~~
15 Christensen et al (2016) found CERES to perform quite well relative to other products, albeit underestimating
16 downwelling LW fluxes from November – February by 10-20 Wm^{-2} relative to in situ observations at Barrow
17 (Alaska). Liu et al (2005) found ISCCP-FD to simulate SW radiative fluxes fairly quite-accurately relative to
18 observations from SHEBA, but to underestimate downwelling SW fluxes in spring by over 30 Wm^{-2} , also
19 overestimating downwelling LW fluxes in winter by around 40 Wm^{-2} . Finally, Lindsay et al (2014) identified
20 ERAI as producing a relatively accurate simulation of surface fluxes compared to in situ observations at Barrow
21 (Alaska) and Ny-Ålesund (Svalbard), although tending to underestimate downwelling SW fluxes in the spring
22 by up to 20 Wm^{-2} and overestimate downwelling LW fluxes in the winter by around 15 Wm^{-2} .

23 In addition to the datasets above, in section 4 we make use of satellite estimates of date of melt onset over sea
24 ice (Anderson et al, 2012), also derived from passive microwave sensors; and in section 5, the CERES-SYN
25 dataset (Rutan et al, 2015), similar to CERES-EBAF but available at higher temporal resolution, is used to
26 examine modelled surface radiation evolution during May in more detail.

27

28 **2.3 – Calculating induced surface flux anomaly**

29 ~~Because the latent heat of sea ice is an order of magnitude greater than the sensible heat required to raise the ice~~
30 ~~to the melting temperature, ice volume is very nearly proportional to the heat required to melt the ice. Ice~~
31 ~~volume therefore acts to integrate the surface and basal energy balance, and is largely determined by the fluxes~~
32 ~~at these interfaces. Across much of the Arctic the sea ice is insulated from the main source of heat energy from~~
33 ~~beneath, the warm Atlantic water layer, by fresh water derived mainly from river runoff (e.g. Serreze et al, 2006;~~
34 ~~Stroeve et al, 2012b). Because of this, although advection-derived ocean heating can be important in setting the~~
35 ~~wintertime ice edge (Bitz et al, 2005), direct solar heating of the ocean is likely to be an order of magnitude~~
36 ~~higher in accounting for basal melting of the sea ice, as observed by Maykut and McPhee, 1995, McPhee et al,~~

2003 and Perovich et al, 2008. Hence the surface energy balance in the Arctic Ocean is of primary importance in controlling the evolution of sea ice volume.

The surface energy balance is composed of four radiative fluxes (downwelling and upwelling SW and LW), two turbulent fluxes (sensible and latent) and of an additional flux due to snowfall. The radiative fluxes dominate in terms of magnitude in both observations (e.g. Persson et al, 2002) and models (the relative magnitude of radiative and turbulent fluxes in HadGEM2-ES is demonstrated in Figure 2). For this reason, and because no large-scale observations of the turbulent fluxes or snowfall exist, in this study we analyse processes affecting only the radiative fluxes.

We express the net radiative flux $F_{SW} + F_{LW}$, where F_{SW} and F_{LW} are fluxes of net surface SW and LW radiation respectively, as functions of key Arctic climate variables using two formulae derived in Appendix A, valid for the ice freezing and melting seasons respectively (as different processes are important depending on the season). The formulae are applied to monthly means of data in model grid cells measuring tens of km across, within which the relevant variables are not necessarily constant or uniform; errors associated with this spatial and temporal extrapolation are briefly discussed in Appendix B.

During the ice freezing season

$$F_{SW} + F_{LW} = \frac{\alpha_{ice} F_{SW\downarrow} + F_{LW\downarrow} + C + BT_b}{1 - B \cdot R_{ice}} \quad (1)$$

where $F_{SW\downarrow}$ and $F_{LW\downarrow}$ are fluxes of downwelling SW and LW radiation respectively, $R_{ice} = \frac{h_I}{k_I} + \frac{h_s}{k_s}$ is the thermal insulance of the ice and snow column (k_I and k_s being ice and snow conductivity respectively, h_I and h_s ice and snow thickness), B is the linearised rate of upwelling longwave dependence on surface temperature at 0°C, T_b ice base temperature in Celsius, C upwelling longwave at 0°C and α_I ice albedo.

During the ice melting season

$$F_{SW} + F_{LW} = F_{LW\downarrow} + C + F_{SW\downarrow} \cdot \left(1 - \alpha_{sea} - a_{ice} (\alpha_{ice} - \alpha_{sea}) - a_{snow} (\alpha_{snow} - \alpha_{ice}) - a_{cold} (\alpha_{cold} - \alpha_{snow}) \right) \quad (2)$$

where α_{sea} , α_{snow} and α_{cold} indicate albedo of open sea, melting snow on sea ice and cold snow on sea ice respectively; a_{snow} and a_{cold} indicate the corresponding area fractions.

(1) and (2) summarises the dependence of surface radiative flux, assumed to account for the major part of the surface flux, on ice thickness, snow thickness, downwelling longwave and shortwave fluxes, ice fraction, snow fraction and melting surface fraction, during the freezing and melting seasons respectively. Hence, at each point

in-space and time, if a model bias in one of these quantities is known, an associated surface flux anomaly can be estimated to first order by multiplying the bias in the quantity by the partial derivative of (1) or (2) with respect to that quantity, calculated at some reference state. For example, given a model anomaly in ice thickness

$(h_i^{MODEL} - h_i^{OBS})$ during the freezing season, a resulting induced surface flux anomaly can be calculated as

$$[\Delta F_{sfc}]_{h_i} \approx (h_i^{MODEL} - h_i^{OBS}) \cdot \frac{\partial F_{sfc}}{\partial h_i} = (h_i^{OBS} - h_i^{MODEL}) \cdot \frac{B}{k_i} \cdot \frac{LW_{down}^{REFERENCE} + BT_b}{(1 - BH_{i_eff}^{REFERENCE})^2} \quad (3)$$

(Here the SW flux is neglected for clarity).

In a similar way, given a model anomaly of melting surface fraction for any point in space and time, an induced surface flux anomaly can be calculated in a similar way to above, by multiplying the model anomaly in melt onset occurrence by the partial derivative of (7) with respect to melt onset occurrence:

$$[\Delta F_{sfc}]_{melt_onset} = (I_{cold}^{MODEL} - I_{cold}^{OBS}) \cdot SW_{down}^{REFERENCE} (\alpha_{cold} - \alpha_{snow}) \quad (4)$$

Using equations (1) and (2), an induced surface flux anomaly due to downwelling SW, downwelling LW, ice thickness, ice fraction and melt onset occurrence was calculated for all model grid cells, for all months in the period 1980-1999. Firstly, a model anomaly in the relevant climate variable was calculated by bilinearly regridding the chosen observational dataset to the model grid, and then averaging this across all dataset years into a climatology. The model bias in the relevant quantity for each grid-cell and model month was then calculated by subtracting this climatology. Secondly, to convert the modelled bias in the relevant quantity to an induced surface flux anomaly, the fields were multiplied by the partial derivative of equation (1) (where modelled $T_{sfc} < -1^\circ C$) or equation (2) (where $T_{sfc} \geq -1^\circ C$). Where observational datasets were available, the reference quantities in the partial derivative fields were calculated as model-observation means. Where no such datasets were available (e.g. for snow thickness), the model field was used. No flux anomalies due to snow thickness or snow fraction were computed, due to a lack of observational datasets with which to calculate model anomaly in these quantities.

3. Evaluating sea ice and surface radiation in HadGEM2-ES

From 1980-1999, the four members of the HadGEM2-ES historically-forced ensemble simulate a mean September sea ice extent of $5.78 \times 10^6 \text{ km}^2$, with ensemble standard deviation of $0.24 \times 10^6 \text{ km}^2$. By comparison, the mean observed September sea ice extent over this period was $6.88 \times 10^6 \text{ km}^2$ according to the HadISST1.2 dataset. Over the reference period, therefore, modelled September sea ice extent is systematically lower than that observed (Figure 23a).

Mean ice thickness is consistently lower than that estimated by PIOMAS for the Arctic Ocean region (Figure 23b), with the highest biases anomalies of -0.4m occurring in October, close to the minimum of the annual cycle, and a near-zero bias anomaly in May, close to the maximum. Modelled ice thickness is also biased low relative to Envisat the ERS satellite measurements (Figure 23c), with thickness biases anomalies ranging from -

1 | ~~1.06~~0.57m in November to ~~-0.72~~16m in April, and relative to the submarine data (Figure 23d), with thickness
2 | ~~biases anomalies~~ ranging from -1.5m in August to -0.8m in January and May. Hence it is very likely that ice
3 | thickness in HadGEM2-ES is biased low in the annual mean, with ~~biases anomalies~~ tending to be higher when
4 | ice thickness is lower. In other words, the ice thickness annual cycle of HadGEM2-ES is likely to be too
5 | amplified, with both anomalously high ice melt during the summer and ice growth during the winter.

6 | Maps of the ice thickness bias in April and October (Figure 23b-d) show agreement that the low ice thickness
7 | bias is smaller on the Pacific side of the Arctic than on the Atlantic side of the Arctic, becoming very small or
8 | even positive in the Beaufort Sea. There is also striking agreement in the spatial pattern of the amplification bias
9 | of the seasonal cycle, as diagnosed by April-October ice thickness difference (Figure 34). All three ice thickness
10 | datasets show the HadGEM2-ES ice thickness seasonal cycle to be too amplified across much of the Arctic, by
11 | up to 1m in the Siberian shelf seas; in addition, all show that in the Beaufort Sea, the amplification is
12 | nonexistent or even negative. There is clear association between areas where modelled annual mean ice
13 | thickness is biased low, and areas where the modelled seasonal cycle is overamplified, and vice versa.

14 | In the following discussion of radiative fluxes, the convention is that positive numbers denote a downwards
15 | flux. Fluxes of downwelling SW radiation are higher in HadGEM2-ES than in all observational estimates during
16 | the spring (Figure 45a-c), with May ~~biases anomalies~~ of 226, 434 and 53 Wm⁻² relative to CERES, ERAI, and
17 | ISCCP-FD respectively. We note that as ERAI and ISCCP-FD have been found to underestimate downwelling
18 | SW during spring at specific locations, the true model ~~bias anomaly~~ is perhaps more likely to lie towards the
19 | lower end of these estimates. During the summer, upwelling SW radiation is consistently lower in magnitude
20 | ~~than in~~ HadGEM2-ES, with June ~~biases anomalies~~ of 164, 373 and 440 Wm⁻² with respect to ERAI, CERES and
21 | ISCCP-FD respectively (a positive ~~bias anomaly~~ in an upward flux demonstrates that the model is too low in
22 | magnitude). There is no consistent signal for a low bias in downwelling SW during the summer, suggesting a
23 | model surface albedo bias. The effect is that modelled net downward SW flux is too large with respect to all
24 | observational datasets in May and June, and with respect to some in July and August. Relative to CERES, the
25 | May downwelling SW bias displays no clear spatial differentiation over the Arctic Ocean (Figure 45a), but the
26 | June upwelling SW bias, and hence the net SW bias, tend to be somewhat higher in magnitude towards the
27 | central Arctic (Figure 45b-c).

28 | Fluxes of longwave (LW) radiation are lower in magnitude in HadGEM2-ES throughout the winter than in all
29 | observational datasets (Figure 45d-f). For downwelling LW, the mean model ~~biases anomalies~~ from December-
30 | April are -165, -22 and -2740 Wm⁻² for ERAI, CERES and ISCCP-FD respectively; for upwelling LW, the
31 | ~~biases anomalies~~ are 11, 165 and 186 Wm⁻² for CERES, ERAI and ISCCP respectively. Because the
32 | downwelling LW ~~biases anomalies~~ vary more than the upwelling LW ~~biases anomalies~~, there is uncertainty in
33 | inferring a model bias in net downwelling LW; ISCCP suggests a large model bias of -224 Wm⁻², CERES a
34 | smaller bias of -11 Wm⁻², while ERAI suggests ~~no a bias of only 1 Wm⁻² at all~~. As in situ studies have shown
35 | both underestimation (by CERES) and overestimation (by ERAI and ISCCP-FD) of downwelling LW in winter,
36 | there is no clear indication as to where the true model ~~bias anomaly~~ in this quantity may lie. Maps of the
37 | downwelling and net down LW bias relative to CERES in February (Figure 45d,f) show the bias tends to be
38 | somewhat higher towards the North American side of the Arctic, and lower on the Siberian side.

Formatted: Superscript

1 In summary, there is evidence of a low bias in net downward LW during the winter, and a high bias in net
2 downward SW during the summer, each of order of magnitude $\sim 10 \text{ Wm}^{-2}$. This is consistent with surface
3 radiation fluxes being the likely first-order cause of the amplified sea ice thickness seasonal cycle. In the next
4 section we describe the process by which surface radiation biases can be attributed to particular model processes
5 by calculating induced surface flux biases, attempt to attribute the surface radiation biases to particular processes
6 using the methodology described in Section 2.

8 4. Calculating induced surface flux bias: Methods

9 In this section, and throughout the rest of the paper, a difference between a model simulation of a particular
10 variable, and any reference dataset for that variable, is referred to as a 'bias'. In a similar way, the difference in
11 model surface flux judged to arise from the difference in a particular variable relative to a reference dataset is
12 referred to as an 'induced surface flux bias'. Attention is drawn to the fact that, due to observational inaccuracy,
13 true model bias relative to the real world may be somewhat different from the biases described in this way.

14 Due to the latent heat of sea ice being an order of magnitude greater than the sensible heat required to raise the
15 ice to the melting temperature, ice volume is very nearly proportional to the heat required to melt the ice. Ice
16 volume therefore acts to integrate the surface and basal energy balance, and is largely determined by the fluxes
17 at these interfaces. Across much of the Arctic the sea ice is insulated from the main source of heat energy from
18 beneath, the warm Atlantic water layer, by fresh water derived mainly from river runoff (e.g. Serreze et al, 2006;
19 Stroeve et al, 2012b). Because of this, in the Arctic Ocean interior direct solar heating of the ocean is likely to
20 be an order of magnitude higher in accounting for basal melting of the sea ice, as observed by Maykut and
21 McPhee, 1995, McPhee et al, 2003 and Perovich et al, 2008, and modelled by Steele et al (2010) and Bitz et al
22 (2005). In particular, it has been found that in HadGEM2-ES oceanic heat convergence is of negligible
23 importance to the sea ice heat budget (Keen et al, 2018). Hence the surface energy balance in the Arctic Ocean
24 is of primary importance in controlling the evolution of sea ice volume.

25 We use a system of well-understood simple models, similar to those used in Thorndike (1992), to estimate, for
26 each model grid cell, and month within the period, the rate at which the surface flux would be expected to
27 change with a particular model variable. For each model grid cell and month, we construct a function

28 $F_{sfc} \approx g_{x,t}(v_1, \dots, v_n) - F_{sfc}$ being surface flux, where the v_i are climate variables that affect the surface flux on
29 timescales shorter than that on which they affect each other, and can therefore be said to be independent for the
30 purposes of this analysis. In this way, at each model grid cell and month the rate at which the surface flux
31 depends on variable v_i can be approximated by $\partial g_{x,t} / \partial v_i$. Given a reference dataset for variable v_i , it then

32 becomes possible to estimate, for each point in time and space, the surface flux bias induced by the bias in v_i as
33 $\partial g_{x,t} / \partial v_i (v_{i,x,t}^{MODEL} - v_{i,x,t}^{REFERENCE})$. The chief advantage of this method is that the resulting fields of induced
34 surface flux bias can then be averaged in time or space to determine the large-scale effects of particular model
35 biases, effectively bypassing nonlinearities in surface flux dependence.

Formatted: Font: (Default) Times New Roman, 10 pt, Bold

Formatted: List Paragraph, Add space between paragraphs of the same style

Formatted: Font: (Default) Times New Roman, 10 pt, Bold

Field Code Changed

Field Code Changed

Field Code Changed

Field Code Changed

Field Code Changed

Field Code Changed

Field Code Changed

Field Code Changed

1 The functions $g_{x,t}$ are constructed as follows. Firstly, a model grid cell in a particular month is classified as
 2 freezing or melting depending upon whether the monthly mean surface temperature is greater or lower than -
 3 2°C. If the grid cell is classified as freezing, the surface flux is approximated as

$$4 F_{sfc} \approx g_{x,t}^w = a_{ice} (F_{atmos-ice} + BT_{ocn}) \sum_{cat} \gamma_{ice-REF}^{cat} (1 - BR_{ice}^{cat})^{-1} + (1 - a_{ice}) F_{atmos-ocean} \quad (1)$$

5 Here $F_{atmos-ice} = F_{LW\downarrow} - \epsilon_{ice} \sigma T_{sfc-REF}^4 + F_{sens-ice} + (1 - \alpha_{ice}) F_{SW\downarrow}$, where a_{ice} is ice area, $F_{LW\downarrow}$, $F_{SW\downarrow}$
 6 and $F_{sens-ice}$ downwelling longwave, shortwave and sensible heat flux respectively, the latter evaluated over
 7 only the ice-covered portion of the grid cell, ϵ_{ice} ice emissivity, $\sigma = 5.67 \times 10^{-8} Wm^{-2} K^{-4}$ the Stefan-
 8 Boltzmann constant, $T_{sfc-REF}$ is monthly mean surface temperature and α_{ice} is mean surface albedo over ice.

9 $F_{atmos-ocean} = F_{LW\downarrow} - \epsilon_{ocn} \sigma T_{ocn}^4 + F_{sens-ocn} + F_{lat-ocn} + (1 - \alpha_{ocn}) F_{SW\downarrow}$, where ϵ_{ocn} is ocean surface
 10 emissivity, T_{ocn} ocean surface temperature (assumed to be -1.8°C), and $F_{sens-ocn}$ and $F_{lat-ocn}$ sensible and
 11 latent heat flux respectively over the ice-free portions of the grid cell. $B = 4\epsilon_{ice} \sigma T_{sfc-REF}^3$ approximates the
 12 local rate of dependence of surface flux on surface temperature, T_b is ice base temperature, γ_{REF}^{cat} is the area of
 13 ice in ice thickness category cat as a fraction of total ice area, where cat ranges from 1 to 5, and

$$14 R_{ice}^{cat} = \frac{h_{ice}^{cat}}{k_I} + \frac{h_{snow}}{k_s}$$

is the thermal insulance of the snow-ice column in category cat , where cat ranges from 1

15 to 5, k_I and k_s being ice and snow conductivity respectively, h_{ice}^{cat} and h_{snow} local ice and snow thickness.

16 If the grid cell is classified as melting, the surface flux is approximated as

$$17 F_{sfc} = g_{x,t}^s = F_{LW\downarrow} - \epsilon_{ice} \sigma T_f^4 + F_{sens} + (a_{ice} \alpha_{ice} + (1 - a_{ice}) \alpha_{ocn}) F_{SW\downarrow} \quad (2)$$

18 where $T_f = 0^\circ C$.

19 The ice surface albedo α_{ice} is further expressed as

$$20 \alpha_{ice} = (\alpha_{melt_ice} - \alpha_{sea}) + I_{snow} (\alpha_{melt_snow} - \alpha_{melt_ice})$$

$$21 + (1 - \gamma_{melt}) (1 - I_{snow}) (\alpha_{cold_ice} - \alpha_{melt_ice}) + (1 - \gamma_{melt}) I_{snow} (\alpha_{cold_snow} - \alpha_{melt_snow}) \quad (3)$$

22 Here $\alpha_{sea} = 0.06$, $\alpha_{melt_ice} = 0.535$, $\alpha_{melt_snow} = 0.65$, $\alpha_{cold_ice} = 0.61$ and $\alpha_{cold_snow} = 0.8$ denote
 23 the parameterised albedos of open water, melting ice, melting snow, cold ice and cold snow respectively, and

Field Code Changed

Field Code Changed

Field Code Changed

Field Code Changed

Field Code Changed

Field Code Changed

Field Code Changed

Field Code Changed

Field Code Changed

Field Code Changed

Field Code Changed

Field Code Changed

Field Code Changed

Field Code Changed

Field Code Changed

Field Code Changed

Field Code Changed

Field Code Changed

Field Code Changed

Field Code Changed

Field Code Changed

Field Code Changed

Field Code Changed

Field Code Changed

Field Code Changed

Field Code Changed

Field Code Changed

Field Code Changed

Field Code Changed

1 γ_{melt} denotes melting surface fraction as a fraction of ice area, while I_{snow} is an indicator for the presence of
2 snow that is set to 1 or 0 depending on whether monthly mean snow thickness exceeds 1mm.

3 The derivation of the formulae is briefly described. The surface flux is composed of four radiative fluxes
4 (downwelling and upwelling SW and LW), two turbulent fluxes (sensible and latent) and of an additional flux
5 due to snowfall (which affects the surface flux as it represents a transfer of negative latent heat, since snow lying
6 on ice changes the enthalpy of the snow-ice system). Hence

7 $F_{sfc} = (1 - \alpha_{ice} F_{SW}) + F_{LW\downarrow} - \epsilon_{ice} \sigma T_{sfc}^4 + F_{sens} + F_{lat} + F_{snowfall}$ is used as a starting point from which the
8 derivation of (2) follows in the melting season, assuming a surface temperature of 0°C and neglecting the
9 snowfall contribution. (3) is designed to mimic the calculation of ice albedo in HadGEM2-ES, which
10 parameterises the effect of meltponds after Curry (2001), reducing albedo linearly as surface temperature rises
11 from -1°C to 0°C. (1) is derived by considering separately the contributions to F_{sfc} from the area of the grid cell
12 covered by each ice category (and by open water). For each ice category, the conductive flux through the ice is
13 assumed to be uniform; the dependence of F_{sfc} on surface temperature is then linearised, using monthly mean
14 surface temperature at each grid point, $T_{sfc-REF}$, as a reference about which to take the linearization. By setting
15 the conductive flux equal to F_{sfc} , the variable T_{sfc} is eliminated. Finally, the contributions to F_{sfc} are
16 multiplied by category ice area and summed. In deriving (1), the contributions of the snowfall flux and of the
17 latent heat flux over ice are neglected.

18 In this way, using equations (1)-(3), we construct the functions $g_{x,t}$, which depend on downwelling LW,
19 downwelling SW, sensible heat flux, category ice thickness, category ice area (freezing cells), total ice area
20 (melting cells), snow thickness, snow area and surface melt onset, variables which have the required property of
21 tending to affect the surface flux on timescales shorter than that on which they affect each other. Hence at each
22 point in space and time the rate of dependence of surface flux on each variable can be approximated by
23 $\partial g_{x,t} / \partial v_i$. We describe for the case of three variables how this process can be used to estimate the surface flux
24 bias induced by biases in that variable, firstly for the variable of melting surface fraction (for simplicity, we
25 describe only the process over grid cells judged to be melting). Model daily surface temperature fields are used
26 to judge, for each month of the year, the average melting surface fraction in each grid cell. The satellite-derived
27 observational estimates of surface melt onset described in Section 2.2 are used to produce a climatology of
28 melting surface fraction for each month and grid cell, and this is subtracted to produce a model bias. This bias is
29 then multiplied by the partial derivative of equation (2) with respect to melting surface fraction,
30 $-F_{SW\downarrow} \left((1 - I_{snow}) (\alpha_{cold_ice} - \alpha_{melt_ice}) + I_{snow} (\alpha_{cold_snow} - \alpha_{melt_snow}) \right)$, evaluated with monthly mean
31 fields of $F_{SW\downarrow}$ and I_{snow} , to produce a monthly mean field of surface flux bias induced by the model bias in
32 melting surface fraction.

Field Code Changed

Field Code Changed

Field Code Changed

Field Code Changed

Field Code Changed

Field Code Changed

Field Code Changed

Field Code Changed

Field Code Changed

Field Code Changed

Field Code Changed

Field Code Changed

Field Code Changed

1 By a similar method, the effect of downwelling LW radiation on surface flux can be estimated, illustrated here
 2 using CERES as a reference dataset (in section 4 below the analysis is performed using multiple datasets) to
 3 produce fields of model bias in downwelling LW radiation. For freezing grid cells, these are then multiplied by

4
$$\frac{\sum_{cat} a_{cat} (1 - BR_{ice}^{cat})^{-1}}{\sum_{cat} a_{cat}}$$
, the partial derivative of (1) with respect to downwelling LW, to produce

5 fields of surface flux bias induced by model bias in downwelling LW. For melting grid cells, the induced
 6 surface flux bias is equal to the downwelling LW bias, as the surface temperature does not change in response to
 7 the bias.

8 The most complex variable to analyse in this way is the ice thickness. Ice thickness strongly affects the surface
 9 flux in the freezing season; thicker ice is associated with less conduction, a colder surface temperature and a
 10 weaker negative surface flux, and hence reduced ice growth. However, it appears in equation (1) only implicitly,

11 in the form of the individual category mean thicknesses \bar{h}_i^{cat} . To use this equation to estimate the effect of ice

12 thickness biases on surface flux, a method of estimating the way biases are distributed amongst thickness

13 categories is needed. Given an estimated model bias in mean thickness \bar{h}_{ice} , it can be argued that the least

14 arbitrary approach is to estimate the model bias in each thickness category to be \bar{h}_{ice} also (i.e. the thickness

15 distribution is uniformly shifted to higher, or lower values). However, this leads to unphysical results at the low

16 end of the distribution; in the case of a negative bias, it implicitly assumes the creation of sea ice of negative

17 thickness; in the case of a positive bias, it assumes that no sea ice of thicknesses between 0m and \bar{h}_{ice} exists.

18 Hence we use a slightly modified approach. The model bias in the lowest thickness category is estimated to be

19 $\bar{h}_{ice}/2$, equivalent to translating the top end of the category by \bar{h}_{ice} but allowing the lower end to remain at 0.

20 The model biases in the other four categories are then estimated to be $\bar{h}_{ice} \frac{a_{ice} - a_1/2}{a_{ice} - a_1}$, i.e. the translation is

21 increased to ensure that the mean ice thickness bias remains correct. Following this, we iterate through the

22 categories, identifying grid cells where the bias is such that a negative category sea ice thickness in the reference
 23 dataset is implied; in these cells, the bias is reduced such that the reference thickness in that category becomes 0,

24 and the bias in the remaining categories is increased proportionally to ensure the mean sea ice thickness bias

25 remains correct.

26 Hence we create, for each category, fields of sea ice thickness bias. These are multiplied by the partial derivative

27 of equation (1) with respect to category ice thickness, $(A + BT_b) a_{cat} (1 - BR_{cat}^{ice})^{-2} \left(\sum_{cat} a_{cat} \right)^{-1}$, to create

28 fields of induced surface flux bias for each category. These are then summed to obtain the total induced surface
 29 flux bias due to ice thickness bias.

30 The process of calculating induced surface flux bias is illustrated in Figure 5 for example months for these three

31 variables. Figure 5a-c illustrates the melt onset analysis. Figure 5a shows the HadGEM2-ES bias in melting

Field Code Changed

Field Code Changed

Field Code Changed

Field Code Changed

Field Code Changed

Field Code Changed

Field Code Changed

Field Code Changed

Field Code Changed

1 surface fraction for the month of June 1980, relative to the NSIDC climatology; the bias is generally positive,
2 reflecting melt onset modelled earlier than observed during this month. Figure 5b shows the field of rate of
3 change of surface flux with respect to melt onset occurrence (effectively downwelling SW multiplied by the
4 difference in parameterised albedos); this tends to be higher in the Central Arctic, reflecting a greater tendency
5 to clear skies here. Finally Figure 5c shows the product of these two fields, the modelled surface flux bias
6 induced by the model bias in melt onset. This is also generally positive, by up to 25 Wm^{-2} in the central Arctic,
7 reflecting the greater absorption of SW radiation induced by the early melt onset.

Formatted: Superscript

8 Figures 5d-f demonstrate the same process for the downwelling LW radiation in January 1980, using CERES as
9 reference dataset. Modelled downwelling LW radiation is seen to be considerably lower in magnitude than that
10 observed by CERES for the 2000-2013 period, by up to 30 Wm^{-2} in many parts of the Central Arctic (Figure
11 2d). The rate of change of surface flux with respect to downwelling LW is shown to be higher (closer to 1) in
12 regions of thinner ice (Figure 2e). This has the result that the induced surface flux bias is greatly reduced
13 relative to the downwelling LW bias in regions of thicker ice (Figure 2f), reflecting the lower efficiency of ice
14 creation in regions of thicker ice; the bias is below 10 Wm^{-2} over much of the Arctic, only approaching 20 Wm^{-2}
15 in the Barents and Kara seas.

Formatted: Superscript

Formatted: Superscript

Formatted: Superscript

16 Figures 5g-i demonstrate the process of calculating surface flux bias induced by the bias in ice thickness in
17 model category 1 (0-0.6m) for the month of January 1980, using PIOMAS as reference dataset. Modelled ice
18 thickness tends to be thinner than estimated by PIOMAS over much of the Arctic for this month, except for an
19 area on the Pacific side of the Arctic; as described above, the bias in category 1 is assumed to be half the total
20 bias. Figure 5h shows the rate of change of surface flux with respect to category 1 ice thickness, which tends to
21 be high in regions where category 1 ice covers higher fractions of the grid cell, generally near the ice edge.

22 **5. Calculating induced surface flux bias: Results**

23 **4. Induced surface flux anomaly**

24 We calculate fields of surface flux anomaly for each month in the model period 1980-1999 induced by model
25 anomalies in downwelling LW, downwelling SW, ice thickness, ice fraction and melt onset occurrence, using in
26 turn CERES, ISCCP-FD and ERAI as reference datasets. The resulting fields are integrated over the Arctic
27 Ocean and averaged over the model period 1980-1999 to produce, for each climate variable, a seasonal cycle of
28 average induced surface flux anomaly. In Figure 6, the seasonal cycles of each component of the surface flux
29 anomaly are shown as a set of stacked barplots, with the results using CERES, ISCCP-FD and ERAI as
30 reference shown from left-right for each month. These are compared, firstly to the net radiative flux anomalies
31 implied by the direct radiation evaluation above (using again CERES, ISCCP-FD and ERAI in turn), and
32 secondly to the sea ice latent heat flux uptake anomaly implied by the ice volume anomalies relative to
33 PIOMAS.

Formatted: List Paragraph, Outline numbered + Level: 1 + Numbering Style: 1, 2, 3, ... + Start at: 1 + Alignment: Left + Aligned at: 0.63 cm + Indent at: 1.27 cm

Formatted: Font: Bold

34 Consistent with the direct radiation comparison and the ice volume anomalies, the induced surface flux
35 anomalies usually sum to positive values during the summer and negative values during the winter. This implies
36 that model biases in the processes investigated tend to cause anomalous ice melt during the summer and
37 anomalous ice growth during the winter. Despite the large discrepancies between the radiative flux estimates of

1 CERES, ISCCP-FD and ERAI, the choice of radiation dataset does not significantly affect any of the induced
2 surface flux anomalies save those due to downwelling SW and LW radiation in the summer, where very large
3 spread is apparent.

4 Induced surface flux anomalies are generally small in May. In June an anomaly of 8 Wm^{-2} is induced by melt
5 onset occurrence; the SSMR observations do not show melt onset to occur in the central Arctic until late June on
6 average, while HadGEM2-ES allows the entire Arctic Ocean to reach the melting temperature by the end of
7 May, inducing a large model anomaly in surface albedo. June also displays a small but growing surface flux
8 anomaly due to ice fraction anomaly, consistent with the anomalously fast ice melt of HadGEM2-ES. By
9 August, although there is no remaining melt onset occurrence anomaly, the surface flux anomaly due to ice
10 fraction is $9-10 \text{ Wm}^{-2}$, allowing the positive surface flux anomaly to be maintained throughout the summer.

11 As noted above, the surface flux anomaly due to downwelling SW and LW radiation varies greatly with the use
12 of observational dataset throughout the summer. Existing in situ validation studies of ERAI (Lindsay et al,
13 2014) and of CERES (Christensen et al, 2016) show both datasets to model downwelling LW accurately to
14 within 15 Wm^{-2} , although CERES is shown to be biased high in June and low in August, while ERAI is biased
15 high in July. Even if these results were representative of the broader Arctic Ocean, it would be hard to interpret
16 the true net effect of the combined LW and SW anomalies, as these will tend to be opposite in sign and of
17 similar orders of magnitude. It is concluded that it is not possible to determine the net effect of downwelling
18 radiative anomalies on surface flux during the summer with current observational data.

19 As the surface of the Arctic Ocean begins to cool in early autumn, a growing negative anomaly due to the now
20 large deficit in ice thickness begins to appear, reaching a maximum of -6 Wm^{-2} in November. The anomaly
21 reduces sharply through the winter as model anomalies in ice thickness with respect to PIOMAS become
22 smaller. From November – April, the downwelling LW induces an additional negative surface flux anomaly,
23 with a mean value of -4 Wm^{-2} indicated from December – February. It is superficially surprising that the choice
24 of radiation dataset does not greatly affect the total induced surface flux, given the large spread in net LW
25 radiation during winter estimated by each dataset. This occurs because in the induced surface flux analysis, the
26 upwelling LW flux anomaly is calculated from other variables, and is therefore strongly anti-correlated with the
27 downwelling LW flux anomaly estimate via the surface temperature.

28 The sum of the induced surface flux anomalies is of a similar shape and order of magnitude to the sea ice latent
29 heat anomalies implied by the thickness anomalies with respect to PIOMAS (Figure 6), with positive anomalies
30 of order 10 Wm^{-2} during the ice melt season, and negative anomalies of order 5 Wm^{-2} during the ice freeze
31 season. The most obvious discrepancy occurs in July, when the sum of the induced surface flux anomalies is
32 small and of indeterminate sign, while a large positive anomaly is implied by the sea ice thickness simulation.
33 This may be due to the ‘missing process’ of surface albedo anomaly due to the presence of snow on sea ice.
34 Early surface melt onset, and sea ice fraction loss, as modelled by HadGEM2-ES, would be expected to be
35 associated also with early loss of snow on sea ice, with an associated surface albedo anomaly, with this process
36 reaching its maximum influence at a time between that of the surface melt onset (June) and that of the sea ice
37 fraction loss (August).

1 In winter the sum of the induced anomalies is consistently lower in magnitude than the sea ice latent heat flux
2 anomaly, indicating that the tendency of model anomalies ice thickness and downwelling LW to cause
3 additional ice growth does not fully account for the anomalous growth seen relative to PIOMAS. This may be
4 due to the use of ice thickness reference dataset; it was noted in Section 2.3 that PIOMAS may underestimate
5 ice thickness in late winter, which would cause the sea ice latent heat flux anomaly, and the surface flux
6 anomaly induced by ice thickness anomalies, to be overestimated and underestimated respectively. It may also
7 indicate that model anomaly in snow thickness, not investigated here, plays a part in inducing additional surface
8 flux anomaly. A third factor in play may be sub-grid scale variation in ice thickness, which as discussed in
9 Appendix B causes an underestimate in the freezing season surface flux anomalies of the order of 10%, or -1
10 Wm^{-2} . It is noted that errors due to sub-monthly scale time covariance in the relevant climate variables,
11 discussed further in Appendix B, are an order of magnitude lower than most absolute values discussed here, and
12 in the context of the large observational uncertainties are unlikely to be important.

13 Using the methods described in Section 4 we calculate surface flux biases induced by model biases in
14 downwelling SW, downwelling LW, ice area, local ice thickness and surface melt occurrence. The resulting
15 fields are averaged over the model period and over the Arctic Ocean region, to produce for each variable a
16 seasonal cycle of surface flux bias induced by the bias in that variable. The induced surface flux (ISF) biases are
17 displayed in Figure 6, together with total ISF bias, radiative flux biases estimated by the direct radiation
18 evaluation relative to ISCCP-FD, CERES and ERAI, and also sea ice latent heat uptake biases implied by the
19 ice thickness biases relative to PIOMAS. The ISF biases are also shown in Table 1, using CERES as reference
20 dataset for the radiative terms.

21 ISF biases tend to sum to negative values during the winter (indicating anomalous modelled energy loss and ice
22 growth) and to positive values during the summer (indicating anomalous modelled energy gain and ice melt),
23 consistent with the radiation and ice thickness evaluation. Major roles are identified for particular processes in
24 certain months. Firstly, in June a bias in surface melt onset induces a surface flux bias of -13.6 Wm^{-2} , equivalent
25 roughly to an extra 11cm of melt. This is associated with the meltpond parameterisation of HadGEM2-ES
26 lowering the surface albedo at the end of May as the surface reaches the melting point, in contrast to SSMI
27 observations which show surface melting to commence on average in mid to late June in the 1980-1999 period.
28 Secondly, in August a bias in ice fraction induces a surface flux bias of 9.6 Wm^{-2} , equivalent to an extra 8cm of
29 melt. This is associated with the overly fast retreat of sea ice in HadGEM2-ES, and the low extents in late
30 summer, as noted in Section 3.

31 Thirdly, the large model biases in downwelling LW present throughout the freezing season induce substantial
32 surface flux biases, ranging from -6.5 to -3.8 Wm^{-2} from October-March (the surface flux biases are
33 considerably lower than the original downwelling LW biases because of the increasing inefficiency by which
34 surface heat loss is converted to sea ice growth as ice thickens). Throughout this period, the total extra heat loss
35 estimated by this process is roughly equivalent ice growth ranging from 20-33cm. Fourthly, the negative biases
36 in ice thickness present at the end of summer also induce substantial surface flux biases which tend to decrease
37 throughout the freezing season as the thickness biases decrease, with an induced surface flux bias of -8.3 Wm^{-2}
38 in November reducing to -2.0 Wm^{-2} in March. This effect is roughly equivalent to an extra 24cm of ice growth.
39 It is noted that while large ISF biases due to downwelling SW and LW are evident during summer, there is very

Formatted: Superscript

Formatted: Superscript

Formatted: Superscript

Formatted: Superscript

Formatted: Superscript

1 large spread in these values between observational datasets, to the extent that the sign of the biases are
2 uncertain. It is concluded that it is not possible to determine the net effect of downwelling radiative biases on
3 surface flux during the summer with current observational data.

4 Internal variability in the ISF biases is measured by taking the standard deviation of the whole-Arctic ISF bias
5 for each process and month across all 20 years in the model period, and all four ensemble members used.
6 Variability is highest in the ice area term, reaching 4.0 Wm^{-2} in July. Variability reaches considerable size in
7 some other terms in some months, for example 1.1 Wm^{-2} for surface melt onset in June, 1.9 Wm^{-2} for ice
8 thickness in November, but is otherwise mainly under 1 Wm^{-2} in magnitude. In each case, therefore, the ISF
9 biases noted above are persistent features of the model.

Formatted: Superscript

Formatted: Superscript

Formatted: Superscript

10 Residuals between the total ISF bias and the directly evaluated radiative flux biases (demonstrated using CERES
11 as radiation reference dataset in Table 1) are comparable in magnitude to the differences between the three
12 different evaluations of the radiative flux biases, indicating that observational uncertainty is likely to dominate
13 uncertainty in the ISF biases themselves. For example, the residual between total ISF bias and net radiation bias
14 varies from -15.4 Wm^{-2} in June to 8.1 Wm^{-2} in November, while the difference between net radiation bias as
15 evaluated by CERES and ERAI respectively varies from -16.9 Wm^{-2} in July to -2.4 Wm^{-2} in September. As
16 discussed in Section 3 above, evidence from in situ validation studies is inconclusive as to the true size of the
17 modelled downwelling LW bias, and hence as to the magnitude of the surface flux bias induced by downwelling
18 LW. On the other hand, the evidence of PIOMAS underestimating winter sea ice thickness suggests that the
19 magnitude of this bias, and the associated ISF bias, may be underestimated. It is also noted that there is a high
20 uncertainty of the order $\pm 10 \text{ Wm}^{-2}$ in the ice area contribution during the winter. This is because the rate of
21 dependence of surface flux on ice area is very high in freezing grid cells (generally $100\text{-}200 \text{ Wm}^{-2}$) due to the
22 large differences between turbulent fluxes over sea ice and open water.

Formatted: Superscript

Formatted: Superscript

Formatted: Superscript

Formatted: Superscript

Formatted: Superscript

Formatted: Superscript

23 In Appendix A potential errors in the ISF analysis are discussed and are found to be quite small in magnitude
24 relative to the difference between observational datasets. Firstly, due to sub-monthly variation in the component
25 variables, the winter downwelling LW component may be underestimated in magnitude by around 0.6 Wm^{-2} on
26 average, and the ice area component in August may be overestimated by around 1.6 Wm^{-2} . Secondly, due to a
27 separate effect by which the ISF biases do not exactly sum to the total surface flux bias, the total bias in October
28 is likely to be overestimated in magnitude by 3.6 Wm^{-2} . Thirdly, due to nonlinearities in the surface flux
29 dependence on ice thickness, the ice thickness component is overestimated in magnitude by 0.7 Wm^{-2} on
30 average from October-April, with a maximum overestimation in November of 1.9 Wm^{-2} . We note that it is
31 possible that in some months the sum of the ISF biases may be a truer representation of the actual surface flux
32 bias than any of the individual evaluations, as the method combines observational estimates with physical
33 relationships between the various flux components. For example, in the satellite datasets observational errors in
34 the different components are not constrained to correlate in a physically realistic sense.

Formatted: Superscript

Formatted: Superscript

Formatted: Superscript

Formatted: Superscript

Formatted: Superscript

35 The most obvious discrepancy between the total ISF bias and the net radiation bias occurs in July, when the sum
36 of the induced surface flux biases is small and of indeterminate sign, while a large positive bias is implied by the
37 sea ice thickness and surface radiation simulations. This may be due to the 'missing process' of surface albedo
38 bias due to the presence of snow on sea ice. Early surface melt onset, and sea ice fraction loss, as modelled by

1 HadGEM2-ES, would be expected to be associated also with early loss of snow on sea ice, with an associated
2 surface albedo bias, with this process reaching its maximum influence at a time between that of the surface melt
3 onset (June) and that of the sea ice fraction loss (August). We note also that the direct effect of thinning ice on
4 ice albedo could induce an additional flux bias relative to the real world, despite the fact that this effect is not
5 modelled in HadGEM2-ES.

6 An annual mean total ISF bias of -3.6 (CERES) and -4.5 Wm⁻² (ERA40) is present when the satellite datasets are
7 used as reference (the annual mean total ISF bias for ERA40 is -0.1 Wm⁻²). It is noted that given a negligible
8 contribution of oceanic heat convergence to the sea ice heat budget in HadGEM2-ES or in the real world, as is
9 argued in Section 4, the annual mean surface flux bias would be expected to be substantially smaller than these
10 figures, as a surface flux bias of -4.5 Wm⁻² is equivalent to a relative thickening of the model sea ice cover by
11 9m over the 1980-1999 period. Analysis of potential sources of error in the ISF calculations in Appendix A
12 does not produce evidence of a systematic bias that could explain these large annual mean negative biases,
13 although the early-winter errors in the ice thickness component could explain a small portion (0.4 Wm⁻²). Given
14 the large discrepancy amongst observational datasets, therefore, it is likely that observational inaccuracy plays a
15 significant part in introducing this annual mean bias.

Formatted: Superscript

Formatted: Superscript

Formatted: Superscript

Formatted: Superscript

Formatted: Font:

16 Spatial patterns in the ISF biases are now discussed. Consistent with the pattern of net SW bias anomaly
17 identified in section 3, the spatial pattern of surface flux bias anomaly induced by melt onset occurrence is
18 characterised by a weak maximum in the central Arctic, with values falling away towards the coast. A more
19 sharply-defined pattern is produced by the ice fraction bias anomaly in August, with high values across the shelf
20 seas and the Atlantic side of the Arctic falling to low or negative values in the Beaufort Sea; the pattern
21 displayed by the ice thickness-induced bias anomaly in November is almost a mirror image. Finally, the surface
22 flux bias anomaly induced by downwelling LW in February displays slightly higher values on the Siberian side
23 of the Arctic than the North American side, the reverse pattern to that displayed by the downwelling LW itself
24 in Figure 54d. The contrast is due to the role the effective ice thickness scale factor plays in determining the
25 induced surface flux -bias anomaly; thicker ice, such as that which tends to be found on the American side of the
26 Arctic in both model and observations, tends to greatly reduce the flux -bias anomaly. This represents the
27 thickness-growth feedback, the reality that thicker ice will grow less quickly than thin ice under the same
28 atmospheric conditions.

29 The spatial patterns of total ISF bias shows many similarities to total net radiation bias evaluated by CERES in
30 most months of the year (Figure 7), notably a tendency in July and August for positive surface flux biases to be
31 concentrated on the Atlantic side of the Arctic, and a tendency throughout the freezing season for negative
32 surface flux biases to be least pronounced in the Beaufort Sea, where the ice thickness biases are likely to be
33 lowest. We note that the spatial pattern of amplification of the ice thickness seasonal cycle displayed in Figure 3
34 is very similar, with amplification most pronounced near the Atlantic Ocean ice edge, and least pronounced in
35 the Beaufort Sea.

36 The surface flux biases anomalies produced by ice fraction biases anomalies in August, and ice thickness
37 biases anomalies in November, provide reasons for the spatial variation in amplification of the ice thickness
38 seasonal cycle seen in Figure 4, as well as the close resemblance of this pattern to the model biases anomalies in

1 annual mean ice thickness. Ice which is thinner in the annual mean will tend to melt faster in summer, due to the
2 net SW ~~biases anomalies~~ associated with greater creation of open water (the ice albedo feedback), and to freeze
3 faster in winter, due to greater conduction of energy through the ice (the ice thickness-growth feedback).

4

5 **5.6. Discussion**

6 The calculation of the surface radiative flux ~~biases anomalies~~ induced by various key processes in the Arctic
7 Ocean produces results qualitatively consistent with the surface radiation evaluation, and with the surface flux
8 ~~biases anomalies~~ implied by the sea ice simulation. Melt onset occurrence and sea ice fraction ~~biases anomalies~~
9 tend to cause anomalous surface warming, and sea ice melt, during the summer, in the HadGEM2-ES historical
10 simulation; downwelling LW and ice thickness ~~biases anomalies~~ tend to cause anomalous surface cooling, and
11 hence sea ice growth, during the winter. ~~It is recognised that it would not be expected that the induced surface~~
12 ~~fluxes would sum to values exactly consistent with either the radiation evaluation, or the sea ice volume~~
13 ~~evaluation, due in the main to observational inaccuracy, but also due to the approximations made when deriving~~
14 ~~the simple models of Section 2.3.~~

15 It is helpful to divide the processes examined into feedbacks (surface flux ~~biases anomalies~~ induced by
16 ~~biases anomalies~~ in the sea ice state itself) and forcings (those induced by downwelling radiative fluxes and melt
17 onset occurrence). In this sense, a ‘forcing’ refers to a variable which is independent of the sea ice volume on
18 short timescales, rather than being used in the traditional sense of a radiative forcing.

19 The surface flux bias induced by biases in ice fraction during the melting season can be identified with the effect
20 of the surface albedo feedback on the sea ice state. This is because during the melting season the ice area affects
21 the estimated surface flux only through the surface albedo, and the surface flux biases induced in this way cause
22 associated biases in ice melt. On the other hand, the surface flux bias induced by biases in ice thickness during
23 the freezing season can be identified with the effect of the thickness-growth feedback on the sea ice state. This is
24 perhaps less obvious, as the ice thickness affects the estimated surface flux via the surface temperature and
25 upwelling LW radiation, while the thickness-growth feedback is usually understood to result from differences in
26 conduction. However, the assumption of flux continuity at the surface in constructing the estimated surface flux
27 means that the cooler surface temperatures, and shallower temperatures gradients occurring for thicker ice
28 categories are manifestations of the same process. Slower ice growth at higher ice thicknesses has a
29 manifestation in a smaller negative surface flux, and the surface temperature is the mechanism by which this is
30 demonstrated. Hence the effect of the thickness-growth feedback is described by the ice thickness-induced
31 component of the surface flux bias.

32 In this way, the ISF analysis allows the effect of the surface albedo and thickness-growth feedbacks on the sea
33 ice state to be quantified, and compared to the effect of other drivers. Arctic-wide, the surface albedo feedback,
34 diagnosed as the ice area-induced component of the surface flux bias, contributes an average of 5.2 Wm^{-2} to the
35 surface flux bias over the summer months, equivalent to an extra 13cm of ice melt; this is very similar to the
36 effect of the surface melt onset-induced component, which contributes an average of 5.3 Wm^{-2} , equivalent also
37 to an extra 13cm of ice melt. In the freezing season, meanwhile, the thickness-growth feedback, diagnosed as
38 the ice thickness-induced component of the surface flux bias, contributes an average of -4.4 Wm^{-2} to the surface

Formatted: Superscript

Formatted: Superscript

Formatted: Superscript

1 flux bias from October-April, equivalent to an extra 26cm of ice freezing, while the downwelling LW-induced
2 component (using CERES as reference dataset) contributes an average of -4.9 Wm^{-2} , equivalent to an extra
3 29cm of freezing over this period.

Formatted: Superscript

4 The biases of the HadGEM2-ES sea ice state can be understood by considering in turn the separate ISF
5 components, their magnitudes, and the times of year when they are important. The surface flux anomaly induced
6 by anomalies in ice fraction can be identified with the surface albedo feedback; that induced by anomalies in ice
7 thickness can be identified with the thickness-growth feedback. The other processes examined—downwelling
8 SW, LW and melt onset occurrence—can be viewed as external forcings. Demonstrated in Figure 7, the
9 anomalous summer sea ice melt is initiated by the early melt onset occurrence, and maintained by the surface
10 albedo feedback, which acts preferentially in areas of thinner ice; the anomalous winter ice growth is maintained
11 both by the thickness-growth feedback (occurring mainly in areas of thinner ice, of greater importance in early
12 winter) and by the downwelling LW ~~bias anomaly~~ (more spatially uniform, in late winter). It is unclear that any
13 significant role is played by the downwelling SW ~~bias anomaly~~, as at the only time of year when the radiation
14 datasets agree that this ~~bias anomaly~~ is of significant value (May), the induced surface flux ~~bias anomaly~~ is more
15 than balanced by that induced by downwelling LW. However this may have a role in causing the later melt
16 onset ~~bias anomaly~~, as discussed below.

17 The means by which the external forcings – anomalous LW winter cooling, and early late spring melt onset –
18 cause an amplified seasonal cycle in sea ice thickness are clear. It is also possible to understand how, in the
19 absence of other forcings, these combine to create an annual mean sea ice thickness which is biased low, as seen
20 in Section 3. The melt onset forcing, by inducing additional ice melting through its effect on the ice albedo, acts
21 to greatly enhance subsequent sea ice melt through the surface albedo feedback. The downwelling LW, on the
22 other hand, by inducing ice freezing, acts to attenuate subsequent sea ice freezing through the thickness-growth
23 feedback. The effect is that surface flux ~~biases anomalies~~ induced by melt onset occurrence are enhanced, while
24 those induced by downwelling LW are diminished.

25 Acting together, the ice thickness-growth feedback and surface albedo feedback create a strong association
26 between lower ice thicknesses and amplified seasonal cycles, because ice which tends to be thinner will both
27 grow faster during the winter, and melt faster during the summer. Hence the melt onset bias, acting alone, would
28 induce a seasonal cycle of sea ice thickness lower in the annual mean, but also more amplified, than that
29 observed, because the surface albedo and thickness-growth feedbacks act to translate lower ice thicknesses into
30 faster melt and growth. For similar reasons, the downwelling LW bias, acting alone, would induce a seasonal
31 cycle of sea ice thickness higher in the annual mean, and also less amplified, than that observed. Hence the melt
32 onset anomaly, acting alone, would induce a seasonal cycle of sea ice thickness both lower, and more amplified,
33 than that observed, while the downwelling LW anomaly acting alone would induce a seasonal cycle of ice
34 thickness higher and less amplified. The bias seen in HadGEM2-ES is a result of the melt onset ~~bias anomaly~~
35 ‘winning out’ over the downwelling LW, due to its occurring at a time of year when the intrinsic sea ice
36 feedbacks render the ice far more sensitive to surface radiation. The anomalously low ice cover in September
37 arises as a consequence of the low annual mean ice thickness, and in particular of the anomalously severe
38 summer ice melt. The finding that the low annual mean ice thickness is driven by surface albedo biases is

1 [consistent with the finding by Holland et al \(2010\) that variance in mean sea ice volume in the CMIP3 ensemble](#)
2 [was mostly explained by variation in summer absorbed SW radiation.](#)

3 The feedbacks of the sea ice state explain the association between spatial patterns of annual mean ice thickness
4 bias and ice thickness seasonal cycle amplification. However, the external forcings (melt onset and downwelling
5 LW bias) cannot entirely explain the spatial patterns in the mean sea ice state biases, because on a regional scale
6 effects of sea ice convergence, and hence dynamics, become more important. The annual mean ice thickness
7 bias seen in HadGEM2-ES is associated with a thickness maximum on the Pacific side of the Arctic, at variance
8 with observations which show a similar maximum on the Atlantic side. It was shown by Tsamados et al (2013)
9 that such a bias could be reduced by introducing a more realistic sea ice rheology.

10 The study would be incomplete without a discussion of possible causes of the two external drivers identified by
11 this analysis as causing sea ice model biases. Underestimation of wintertime downwelling LW fluxes [in the](#)
12 [Arctic](#) is known to be a widespread model bias in the CMIP5 ensemble (e.g. Boeke and Taylor, 2016). Pithan et
13 al (2014) showed that this bias was likely to be a result of insufficient liquid water content of clouds forming in
14 subzero air masses, resulting in a failure to simulate a particular mode of Arctic winter climate over sea ice; the
15 'mild mode', characterised by mild surface temperatures and weak inversions, whose key diagnostic is observed
16 to be a net LW flux of close to 0 Wm^{-2} (Stramler et al, 2011; Raddatz et al, 2015 amongst others). HadGEM2-
17 ES was not one of the models assessed by Pithan et al (2014), but its winter climate simulation displays many of
18 the characteristic biases displayed by these, notably a tendency to model very low cloud liquid water fractions
19 during winter compared to MODIS observations (Figure 8a) and a failure to simulate the milder mode of Arctic
20 winter climate as demonstrated in SHEBA observations, diagnosed by 6-hourly fluxes of net LW (Figure 8b).
21 Here we conclude that a similar mechanism is likely to be at work in HadGEM2-ES, and that insufficient cloud
22 liquid water is the principal driver of the anomalously low downwelling LW fluxes.

23 The causes of the early melt onset bias of HadGEM2-ES are harder to determine. For most of the spring,
24 comparison of daily upwelling LW fields of HadGEM2-ES to CERES-SYN observations (not shown) shows the
25 Arctic surface to be anomalously cold in the model, as during the winter. During May, however, upwelling LW
26 values rise much more steeply in the model, and surface melt onset commences during mid-to-late May, far
27 earlier than in the satellite observations. A possible cause of the overly rapid surface warming during May is the
28 zero-layer thermodynamics approximation used by HadGEM2-ES, in which the ice heat capacity is ignored.
29 Comparing fields of surface temperature in HadGEM2-ES between the beginning and the end of May shows a
30 'missing' ice sensible heat uptake flux of $10\text{-}30 \text{ Wm}^{-2}$ over much of the central Arctic, which would in turn be
31 associated with a reduction of flux into the upper ice surface of $5\text{-}15 \text{ Wm}^{-2}$. Examination of modelled and
32 observed daily timeseries of downwelling LW and net SW fluxes in late May and early June suggests that a
33 surface flux reduction of this magnitude could delay surface melt by up to 2 weeks, a substantial part of the
34 modelled melt onset [bias anomaly](#)-seen.

35 Another cause of the rapid warming may be the increasing relative magnitude of the downwelling SW response
36 to cloud [biase anomalies](#) as May progresses (compared to the downwelling LW response). Comparison of 5-
37 daily means of HadGEM2-ES radiative fluxes during May to those from the CERES-SYN product (not shown)

Formatted: Superscript

Formatted: Superscript

1 support this hypothesis; a modelled bias anomaly in downwelling SW grows quickly during early May, from ~
2 0Wm^{-2} to $\sim 30\text{Wm}^{-2}$, while the modelled bias anomaly in downwelling LW remains roughly constant.

3 The ISF analysis as presented does not comprise an exhaustive list of processes affecting Arctic Ocean surface
4 fluxes. The missing processes of the effects of snow fraction and ice thickness bias on the surface albedo have
5 already been noted; the effect of snow thickness bias on winter conduction and surface temperature is another
6 such process which cannot be included due to inadequate observations. Model biases in the turbulent fluxes may
7 also be significant; while the process which is likely most important in determining these during the winter is
8 captured (ice fraction in the freezing season), a more detailed treatment of turbulent fluxes would also examine
9 the effect on these of the overlying atmospheric conditions. It is also noted that snowfall itself is a component of
10 the surface flux which could in theory be evaluated directly given a sufficiently reliable observational reference.

11 Finally, it is noted that a complete treatment of model biases affecting the sea ice volume budget would also
12 examine causes of bias in oceanic heat convergence. For the reasons discussed in Section 4 these are likely to be
13 small in the Arctic Ocean interior in HadGEM2-ES and observations, but the model bias could nevertheless
14 conceivably be of considerable size in the context of the surface flux biases shown in Figure 6. The total Arctic
15 Ocean heat convergence modelled by HadGEM2-ES for the period 1980-1999 is 4.4Wm^{-2} , although this figure
16 shows high sensitivity to the location of the boundary in the Atlantic sector, suggesting that most of this heat is
17 released close to the Atlantic ice edge. This figure is slightly higher than the 3Wm^{-2} found by Serreze et al
18 (2007) in their analysis of the Arctic Ocean heat budget, but is broadly consistent with observational estimates
19 of oceanic heat transport through the Fram Strait (likely to be the major contributor to Arctic Ocean heat
20 convergence) from 1997 to 2000 by Schauer et al, 2004. This suggests that errors in oceanic heat convergence
21 are unlikely to contribute significantly to sea ice volume biases in HadGEM2-ES. However, for a hypothetical
22 model which simulated greater oceanic heat convergence in the Arctic Ocean interior, the surface flux analysis
23 presented here would fail to adequately describe the model bias in the sea ice volume budget.

Formatted: Not Highlight

26 6.7. Conclusions

27 HadGEM2-ES simulates a sea ice cover which is not extensive enough at annual minimum. Comparison to
28 various ice thickness datasets shows that it also has too low an annual mean ice thickness, and that its ice
29 thickness seasonal cycle is likely to be overamplified. Evidence of a positive net SW bias during the ice melt
30 season, and a negative net LW bias during the ice freezing season is apparent from evaluations using multiple
31 radiation datasets.

32 An evaluation of processes influencing surface radiation, combined with simple models to estimate their effect,
33 produces results consistent with the evaluation of the sea ice state and surface radiation; processes tend to cause
34 anomalous ice melt during the melting season, and anomalous ice growth during the freezing season.

35 Consequently model biases anomalies in sea ice growth and melt rate can be attributed in detail to different
36 causes; in particular, the roles played by the sea ice albedo feedback, by the sea ice thickness-growth feedback,
37 and by external forcings, can be quantified. The analysis reveals how the melt onset bias anomaly of HadGEM2-

1 ES tends to make model ice thickness both low in the annual mean, and too amplified in the seasonal cycle, with
2 the downwelling LW ~~bias anomaly~~ acting to mitigate both effects. The result is consistent with the prediction of
3 DeWeaver et al (2008) that sea ice state is more sensitive to surface forcing during the ice melt season than
4 during the ice freeze season. The analysis also suggests that through an indirect effect on surface albedo at a
5 time when sea ice is particularly sensitive to surface radiation- ~~biases anomalies~~, the zero-layer approximation,
6 which was until recently commonplace in coupled models, may be of first-order importance in the sea ice state
7 bias of HadGEM2-ES.

8 ~~The analysis also makes explicit the link between the spatial pattern of anomalies in annual mean ice thickness,
9 and anomalies in the April-October ice thickness difference. Regions where ice thickness tends to be biased
10 particularly low in the annual mean also display higher amplification in the seasonal cycle, due to the direct
11 action of the thickness-growth and ice albedo feedbacks, despite the initiating factors of melt-onset occurrence
12 and downwelling LW anomaly being comparatively spatially uniform. However, the reasons for the underlying
13 spatial distribution of the annual mean ice thickness anomalies in HadGEM2-ES are likely to lie in ice dynamics
14 rather than thermodynamics.~~

15 A clear link has been demonstrated between the spatial pattern of biases in annual mean ice thickness, likely
16 driven by ice dynamics, and that of biases in the April-October thickness. Where ice thickness is biased low in
17 the annual mean, an enhanced seasonal cycle is apparent. This is due to the thickness-growth and ice albedo
18 feedbacks, initiated by melt early melt onset and downwelling LW bias, both of which are spatially uniform.

19 ~~The method is limited by the current inability to evaluate the impact of anomalies in modelled snow cover, as
20 well as by the large observational uncertainties in summer surface radiation, underlying the importance of
21 reducing uncertainty in large-scale observations of Arctic climate variables. Adding in the 'missing processes'
22 of freezing season snow thickness, and melt season snow fraction, would represent useful extensions to the
23 analysis presented. Other potential causes of SEB anomalies not investigated in this study include processes
24 causing anomalies in the turbulent fluxes, and in particular the effects of anomalies in sea ice fraction during the
25 freezing season.~~

26 Large observational uncertainties for snow cover and summer surface radiation limit the overall accuracy of the
27 methodology presented here. The addition of freezing season snow thickness, and melt season snow fraction,
28 would represent useful extensions to the analysis presented. An additional caveat regarding this analysis is that it
29 does not consider factors influencing turbulent fluxes (with the exception of the ice area, but this contribution is
30 subject to particularly high uncertainty). It also does not consider the influence of oceanic heat convergence on
31 sea ice state; in HadGEM2-ES the latter is small (~10%), but might be more significant in other models.

32 In the case study presented here, the analysis provides mechanisms behind a model bias in sea ice simulation.
33 However, the analysis could also be used to investigate a sea ice simulation that was ostensibly more consistent
34 with observations, to determine whether or not the correct simulation was the consequence of model biases that
35 cause opposite errors in the surface energy budget; a negative result would greatly increase confidence in the
36 future projections of such a model. The analysis could be also used to investigate a whole model ensemble, to
37 attribute spread in modelled sea ice state to spread in the underlying processes affecting the SEB, focussing

Formatted: Line spacing: 1.5 lines

Formatted: Font: Times New Roman,
10 pt

1 attention on ways in which spread in modelled sea ice could be reduced. It is noteworthy that Shu et al (2015)
 2 found the CMIP5 ensemble mean Arctic sea ice volume to be biased low in the annual mean, and overamplified
 3 in the seasonal cycle, relative to PIOMAS (albeit over the entire Northern Hemisphere), suggesting that the
 4 behaviour exhibited by HadGEM2-ES may be quite common in this ensemble.

5 Finally, it is suggested that the ISF method, as well as being used to compare a model to observations, could
 6 also be used to understand the reasons for the biases of one model with respect to another. Such a comparison
 7 would avoid the issues of observational uncertainty discussed above, enabling the contributions of the different
 8 model variables to the surface flux biases to be evaluated more accurately.

9 **Appendix A: Derivation of formulae used for surface flux analysis**

10 The surface energy balance equation over an area of sea ice and open water, in which fluxes arriving at the
 11 surface from above are equated with fluxes of energy into the ice and ocean below, can be expressed as follows,
 12 ignoring the contribution from snowfall occurring on both sides:

$$13 \quad F_{SW} + F_{LW} + F_{sens} + F_{lat} = F_{cond} + F_{melt} + F_{sublim} + F_{wat} \quad (A1)$$

14 Here F_{SW} , F_{LW} , F_{sens} , F_{lat} , F_{cond} , F_{melt} , F_{sublim} and F_{wat} refer to fluxes of net SW, LW, sensible and
 15 latent heat flux, conductive heat flux into sea ice, top melting flux into sea ice, sea ice net sublimation flux, and
 16 flux of energy directly into seawater. Here and below, the convention used is that positive numbers denote
 17 downward fluxes. For the reasons given above, we neglect the turbulent heat fluxes. By implication we also
 18 neglect the sea ice net sublimation flux. Hence the surface flux is equated with $F_{SW} + F_{LW}$.

19 During the ice freezing season, surface temperatures are below freezing, conduction into the ice is substantial,
 20 and $F_{melt} = 0$. In addition, ice fraction tends to be close to 1 over much of the Arctic. We assume for the
 21 purposes of this analysis that ice fraction during the freezing season is equal to 1 (equivalent to neglecting F_{wat}
 22), while recognising that due to turbulent fluxes being observed to be very large in regions of open water, F_{wat}
 23 may in reality be of significant size. In the following analysis, as a result, the effects of model anomalies in ice
 24 fraction during the freezing season on the surface flux are not estimated.

25 Linearising the dependence of $F_{SW} + F_{LW}$ on the surface temperature T_{sfc} about the freezing point as
 26 $A + BT_{sfc}$, and assuming uniform conduction within the ice (thereby ignoring sensible heating of ice), we have

$$27 \quad A + BT_{sfc} = \frac{T_{sfc} - T_b}{R_{ice}} \quad (A2)$$

28 where the ice thermal insulance $R_{ice} = h_I/k_I + h_S/k_S$, h_I , h_S , k_I and k_S being ice and snow thickness, and
 29 ice and snow conductivity, respectively.

1 Solving for T_{sfc} and re-substituting, we have

$$2 \quad F_{SW} + F_{LW} = \frac{A + BT_b}{1 - B \cdot R_{ice}} \quad (A3)$$

3 A represents the surface temperature-independent part of the surface flux, and can be identified with

4 $F_{SW} + F_{LW\downarrow} + C$, where $F_{LW\downarrow}$ is the downwelling LW flux and C is the upwelling longwave flux associated
5 with a surface temperature of 0°C . Hence

$$6 \quad F_{sfc} = \frac{\alpha_l F_{SW\downarrow} + F_{LW\downarrow} + C + BT_b}{1 - B \cdot R_{ice}} \quad (A4)$$

7 Equation (A4) summarises the dependence of the net radiative flux on downwelling radiative fluxes and on ice
8 and snow thickness, and is equivalent to equation (1), used to calculate induced surface flux anomaly during the
9 freezing season.

10 During the ice-melting season, conductive flux is near zero, surface temperature is close to 0°C throughout, and
11 ice fraction is no longer necessarily close to 1. Hence the surface flux is

$$12 \quad F_{sfc} = F_{LW\downarrow} + C + \alpha_s F_{SW\downarrow} \quad (A5)$$

13 where α_s is surface albedo and $C = \epsilon\sigma T_f^4$ is upwelling longwave radiation at $T_f = 0^\circ\text{C}$. In HadGEM2-ES,
14 surface albedo is parameterised after Curry et al (2001), which approximates the effect of sea ice meltponds by
15 reducing albedo as the surface temperature approaches the melting point. Surface albedo is therefore affected by
16 ice fraction, the presence or otherwise of snow, and whether or not melt-onset has occurred. The effect can be
17 summarised as

$$18 \quad F_{sfc} = F_{LW\downarrow} + C + F_{SW\downarrow} \cdot \left(1 - \alpha_{sea} I_{ice} (\alpha_{ice} - \alpha_{sea}) - I_{snow} (\alpha_{snow} - \alpha_{ice}) - I_{cold} (\alpha_{cold} - \alpha_{snow})\right)$$

$$19 \quad (A6).$$

20 where α_{sea} , α_{ice} , α_{snow} and α_{cold} indicate the modelled albedos of open water, bare ice, melting snow and
21 cold snow respectively, and I_{ice} , I_{snow} and I_{cold} indicate the presence of sea ice, snow cover and cold snow
22 (that is far from the melting point) respectively. Integrated over large areas, I_{ice} becomes ice area fraction a_{ice}
23 (and similarly for I_{snow} and I_{cold}), giving equation (2), used to calculate induced surface flux anomaly during
24 the melting season.

25

26 **Appendix B: Error associated with spatial and temporal extrapolation**

The application of equations (A4) and (A6) to monthly means of data valid for grid cells tens of km across introduces two potential sources of error in estimating the surface flux anomaly induced. Firstly, subgrid-scale variation in ice thickness, which is not accounted for by the simple model, tends to increase the efficiency of heat loss and hence ice creation during the freezing season via the scale factor $\frac{1}{1 - Bh_{i_eff}}$, rendering ice growth more sensitive to errors in the forcing variable. In an analysis of a field of category ice thickness produced by HadGEM2-ES for January 1994, this was found to cause an average underestimate of 8% in the scale factor value, and hence the induced surface flux anomaly.

Secondly, error will occur due to covariance in time between variables being multiplied. As both melt-onset occurrence and ice fraction observations were available on daily timescales, the effect of this covariance was assessed by calculating induced surface flux anomaly due to melt onset occurrence and ice fraction on both daily and monthly timescales. The daily covariance was found to cause a maximum error of 0.1 Wm^{-2} in the melt onset induced anomaly, in June, and of 0.5 Wm^{-2} in the ice fraction induced anomaly, in August, with most other monthly anomalies being below 0.1 Wm^{-2} .

Appendix A: Analysis of potential errors in ISF bias calculation

Due to observational uncertainty, it is difficult to directly evaluate the ISF bias calculations. Instead, we examine in turn the two principal sources of error in the method; firstly, error in correctly characterising the dependence of surface flux on a climate variable, and secondly, error in approximating the surface flux bias induced by this as the product of the surface flux dependence with the model bias in that variable.

To analyse the first source of error, we begin by comparing fields of the approximated surface flux $g_{x,t}$ to those of the real modelled surface flux F_{sfc} . The $g_{x,t}$ are found to capture well the large-scale seasonal and spatial variation in surface flux, but are prone to systematic errors which vary seasonally, indicated in Figure A1; firstly, a tendency to underestimate modelled negative surface flux in magnitude from October-April by 13% on average; secondly, a tendency to overestimate modelled positive surface flux from June-August by up to 10 Wm^{-2} ; thirdly, during May, a underestimation varying from $5\text{-}20 \text{ Wm}^{-2}$.

Examining first the winter underestimation (demonstrated in Figure A1 a-c), it is found that for each model month the relationship between estimated and actual surface flux is strongly linear, with underestimation factors ranging from $6 \pm 1\%$ in December to $17 \pm 2\%$ in April. This suggests that the cause lies in systematic

underestimation of the scale factor $\sum_{cat} \gamma_{ice-REF}^{cat} (1 - BR_{ice}^{cat})^{-1}$. A possible cause is covariance in time between

$\gamma_{ice-REF}^{cat}$ and R_{ice}^{cat} within each month, particularly in the first ice category; during the freezing season,

occurrence of high fractions of ice in category 1, the thinnest category, would be expected to be associated with formation of new ice, and correspondingly lower mean thicknesses of ice in this category, lower values of R_{ice}^{cat}

Formatted: Line spacing: 1.5 lines

Field Code Changed

Field Code Changed

Field Code Changed

Field Code Changed

Field Code Changed

Field Code Changed

Field Code Changed

1 and higher values of $(1 - BR_{ice}^{cat})^{-1}$. A calculation using daily values of $\gamma_{ice-REF}^{cat}$ ranging from 0.1 – 0.5, and
2 daily values of h_j^{cat} ranging from 0.2 – 0.5m, predicts that this effect would in this case lead to an
3 underestimation of 9% in the magnitude of the surface flux, sufficient to explain all of the underestimation in
4 October, December and January, and most in November, February and March. This effect would produce a
5 corresponding underestimation of the rate of dependence of surface flux on downwelling LW radiation and ice
6 thickness throughout the freezing season. It was estimated that the downwelling LW component of the ISF bias
7 is underestimated by 0.6 Wm^{-2} for the freezing season on average due to this effect.

Field Code Changed

Field Code Changed

Field Code Changed

8 Secondly, we examine the tendency to overestimate surface flux during the summer (Figure A1d-f), an effect
9 that displays a spatially uniform bias rather than a spatially uniform ratio, ranging from $5\text{-}15 \text{ Wm}^{-2}$ in July and
10 August; the bias is smaller, and in the central Arctic negative, during June. A possible contributing factor to this
11 bias is within-month covariance between ice area and downwelling SW; during July and August, both
12 downwelling SW and surface albedo fall sharply, an effect that would tend cause the monthly mean surface flux
13 to be overestimated. To estimate this effect, monthly trends in these variables were estimated by computing half
14 the difference between modelled fields for the following and previous month. For July, an overestimation in
15 surface flux of magnitude $5\text{-}15 \text{ Wm}^{-2}$ was indeed predicted in the Siberian seas, as well as the southern Beaufort
16 and Chukchi Seas; however, in the central Arctic no overestimation was predicted, due to near-zero trends in ice
17 area in the summer months. It is possible that some covariance between ice area and downwelling SW is
18 nevertheless present in these regions, due to enhanced evaporation and cloud cover in regions of reduced ice
19 fraction.

Formatted: Superscript

Formatted: Superscript

20 However, this effect would have no direct impact on the ISF biases because these are computed from monthly
21 means of the model bias in one variable by the model mean in the other; hence, it is covariance between bias
22 and mean that would induce inaccuracy in this case. By similarly approximating the trend in monthly mean
23 model bias as half the difference between model bias in the adjacent months, the error in downwelling SW and
24 ice area contributions were evaluated. Error in the downwelling SW term was found to be significant early in the
25 summer, with an error of -2.7 Wm^{-2} in June; error in the ice area term was found to be significant later in the
26 summer, with errors of -1.7 Wm^{-2} and -1.6 Wm^{-2} in July and August respectively. However, the August error is
27 small relative to the total ISF bias identified.

Formatted: Superscript

Formatted: Superscript

Formatted: Superscript

Formatted: Superscript

28 Thirdly, we examine the reasons for the underestimation of surface flux in May (Figure A1g-i), a pattern unique
29 to this month which is seen to be small in the central Arctic but to approach 20 Wm^{-2} at the Arctic Ocean coasts.
30 A likely cause of this inaccuracy is the classification of grid cells as ‘freezing’ or ‘melting’ for entire months.
31 During May, as has been seen, most model grid cells in fact cross from one category to the other; however,
32 virtually all Arctic Ocean grid cells are classified as freezing for the month as a whole. The difference field
33 between estimated ‘freezing surface flux’ and ‘melting surface flux’ is similar in magnitude and in spatial
34 pattern to the underestimation field, being near-zero in the central Arctic but rising to 25 Wm^{-2} close to the
35 Arctic Ocean coasts. It is concluded that the actual model mean surface flux is much higher than that estimated
36 near the coast due to these grid cells experiencing melting conditions from relatively early in the month.
37 Although this error is not directly relevant to the results of this paper, as no unequivocal ISF biases were

Formatted: Superscript

Formatted: Superscript

1 identified for May, it would have the potential to lead to overestimation of the dependence of surface flux on ice
 2 thickness, and underestimation of dependence on all other variables, as the upwelling LW flux is unable to
 3 counteract changes in surface forcing once the surface has hit the melting point.

4 Having examined potential causes of error in estimating dependence of surface flux on individual variables, the
 5 validity of estimating ISF biases as the product of these with model variable biases is now discussed. Even if the
 6 dependence of monthly mean surface flux on variable v_i at a model grid cell is perfectly described by

7 $\partial g_{x,t} / \partial v_i$ that dependence changes as the realisation varies from the model state to the real-world state. As a
 8 simplified example, a component of the surface flux, net SW, is equal to $F_{SW\downarrow} (1 - \alpha_{sfc})$, and induced surface

9 flux biases due to model biases in $F_{SW\downarrow}$ and α_{sfc} would be calculated as $F'_{SW\downarrow} (1 - \alpha_{sfc}^{mod})$ and $F_{SW\downarrow}^{mod} \alpha'_{sfc}$
 10 respectively. However, the sum of the two induced surface flux biases will not be exactly equal to the true
 11 surface flux bias, $F_{SW\downarrow}^{mod} (1 - \alpha_{sfc}^{mod}) - F_{SW\downarrow}^{obs} (1 - \alpha_{sfc}^{obs})$, but will differ from it by $F'_{SW\downarrow} \alpha'_{sfc}$. This is due to the
 12 dependencies being evaluated on model states which are themselves biased.

13 This apparent problem can be resolved only by viewing the ISF method as a way not simply of estimating model
 14 biases due to a particular variable, but of characterising them, i.e. by accepting that the quantity that we are
 15 trying to estimate is itself somewhat subjective. Instead of requiring the ISF method to be correct, it is required
 16 that it gives useful, physically realistic results. In the case given above, a sufficient condition is that $F'_{SW\downarrow} \alpha'_{sfc}$
 17 is small relative to $F'_{SW\downarrow} (1 - \alpha_{sfc}^{mod})$ and $F_{SW\downarrow}^{mod} \alpha'_{sfc}$, i.e. that the model bias in both downwelling SW and in
 18 surface albedo is small relative to the absolute magnitudes of these variables.

19 More generally, the difference between the surface flux bias F'_{sfc} and the sum of the induced surface flux biases

20 $\sum_i v'_i \partial g_{x,t} / \partial v_i$ can be approximated by $\sum_{\substack{i,j \\ i \neq j}} v'_i v'_j \partial^2 g_{x,t} / \partial v_i \partial v_j$, a term that can be calculated relatively

21 easily as many of the derivatives go to zero. Averaged over the Arctic Ocean this term was small in most
 22 months of the year, but of significant size in October (3.6 Wm^{-2}), due to co-location of substantial negative
 23 biases in downwelling LW and category 1 ice thickness in this month, indicating that the true surface flux bias
 24 in this month may be substantially smaller (in absolute terms) than the -11.5 Wm^{-2} obtained from summing the
 25 ISF biases.

26 Finally, the induced surface flux calculation implicitly assumes a linear dependence of surface flux on each
 27 climate variable. However, this is not the case for the ice thickness, where higher-order derivatives do not go to
 28 zero, and in some regions of thinner ice actually diverge. It is possible to quantify the error introduced by the

29 assumption of linearity by comparing the partial derivative $(A + BT_b) a_{cat} (1 - BR_{cat}^{ice})^{-2} \left(\sum_{cat} a_{cat} \right)^{-1}$ to the

Field Code Changed

Field Code Changed

Field Code Changed

Field Code Changed

Field Code Changed

Field Code Changed

Field Code Changed

Field Code Changed

Field Code Changed

Field Code Changed

Field Code Changed

Field Code Changed

Field Code Changed

Field Code Changed

Field Code Changed

Formatted: Superscript

Formatted: Superscript

Field Code Changed

1 quantity $(A + BT_b)a_{cat}(1 - BR_{cat}^{ice})^{-1}(1 - BR_{cat}^{ice-REF})^{-1}\left(\sum_{cat} a_{cat}\right)^{-1}$, where $R_{cat}^{ice-REF} = h_I^{OBS}/k_I + h_S/k_S$,
 2 h_I^{OBS} being climatological ice thickness in the reference dataset, in this case PIOMAS, and all other terms
 3 defined as in Section 4. It can be shown that multiplying this quantity by the model bias produces the exact bias
 4 in estimated surface flux that is being approximated by $\partial g_{x,i}/\partial h_I(h_I^{MODEL} - h_I^{OBS})$. Hence the bias in the ice
 5 thickness component induced by the nonlinearity can be calculated directly. It is found that the nonlinearity
 6 causes the ice thickness component to be overestimated in magnitude by 0.7 Wm^{-2} on average from October-
 7 April, with a maximum overestimation of 1.9 Wm^{-2} in November.

Field Code Changed

Field Code Changed

Field Code Changed

Field Code Changed

Formatted: Superscript

Formatted: Superscript

9 Code availability

10 The code used to create the fields of induced surface flux bias is written in Python and is provided as a
 11 supplement (directory 'ISF'). The code used to create Figures 1-8, as well as Figure A1, is also provided
 12 in Python and is provided as a supplement (directory 'Figures'). In addition, the routines used to estimate errors
 13 in the ISF analysis are provided create the monthly induced surface flux anomaly fields used in Figures 6&7
 14 from the basic model and observation fields is provided (directory 'Analysis'). Finally, the code used to create
 15 Table 1 is provided (directory 'Tables'). A set of auxiliary routines used by most of the above are also provided
 16 (directory 'Library'). Most routines make use of the open source Iris library, and several make use of the open
 17 source Cartopy library.

19 Data availability

20 Monthly mean ice thickness, ice fraction, snow thickness and surface radiation, as well as daily surface
 21 temperature and surface radiation, for the first historical member of HadGEM2-ES, is available from the CMIP5
 22 archive at https://cmip.llnl.gov/cmip5/data_portal.html.

23 NSIDC ice concentration and melt onset data can be downloaded at <http://nsidc.org/data/NSIDC-0051> and
 24 <http://nsidc.org/data/NSIDC-0105> respectively.

25 PIOMAS ice thickness data can be downloaded at [http://psc.apl.uw.edu/research/projects/arctic-sea-ice-volume-](http://psc.apl.uw.edu/research/projects/arctic-sea-ice-volume-anomaly/data/)
 26 [anomaly/data/](http://psc.apl.uw.edu/research/projects/arctic-sea-ice-volume-anomaly/data/).

27 ERAI surface radiation data can be downloaded at [http://apps.ecmwf.int/datasets/data/interim-full-](http://apps.ecmwf.int/datasets/data/interim-full-daily/levtype=sfc/)
 28 [daily/levtype=sfc/](http://apps.ecmwf.int/datasets/data/interim-full-daily/levtype=sfc/).

29 ISCCP-FD surface radiation data is available at https://isccp.giss.nasa.gov/projects/browse_fc.html.

30 CERES surface radiation data is available at [https://climatedataguide.ucar.edu/climate-data/ceres-ebaf-clouds-](https://climatedataguide.ucar.edu/climate-data/ceres-ebaf-clouds-and-earths-radiant-energy-systems-ceres-energy-balanced-and-filled)
 31 [and-earths-radiant-energy-systems-ceres-energy-balanced-and-filled](https://climatedataguide.ucar.edu/climate-data/ceres-ebaf-clouds-and-earths-radiant-energy-systems-ceres-energy-balanced-and-filled).

33 Acknowledgements

34 This study was supported by the Joint UK BEIS/Defra Met Office Hadley Centre Climate Programme
 35 (GA01101). This work was supported by the Joint UK BEIS/Defra Met Office Hadley Centre Climate

Formatted: Font: (Default) Times New Roman, 10 pt

1 [Programme \(GA01 101\), and the European Union's Horizon 2020 Research & Innovation programme through](#)
2 [grant agreement No. 727862 APPLICATE.](#)

3 ▲ -----
4 Thanks are due to Richard Wood and Ann Keen for helpful comments on multiple versions of this study.

6 References

7 Anderson, M., Bliss, A. and Drobot, S.: Snow Melt Onset Over Arctic Sea Ice from SMMR and SSM/I-SSMIS
8 Brightness Temperatures, Version 3. Boulder, Colorado USA. NASA National Snow and Ice Data Center
9 Distributed Active Archive Center. doi: <http://dx.doi.org/10.5067/22NFZL42RMUO> [accessed October 2015],
10 2001, updated 2012

11 Bitz, C. M. and Roe, G. H.: A Mechanism for the High Rate of Sea Ice Thinning in the Arctic Ocean, *J. Clim.*,
12 17, 18, 3623–3632, doi: [https://doi.org/10.1175/1520-0442\(2004\)017](https://doi.org/10.1175/1520-0442(2004)017), 2004

13 Bitz, C. M., Holland, M. M., Hunke, E. C., and Moritz, R. M.: Maintenance of the Sea-Ice Edge, *J. Clim.*, 18,
14 15, 2903–2921, doi: <https://doi.org/10.1175/JCLI3428.1>, 2005

15 Bitz, C. M.: Some Aspects of Uncertainty in Predicting Sea Ice Thinning, in *Arctic Sea Ice Decline:*
16 *Observations, Projections, Mechanisms, and Implications* (eds E. T. DeWeaver, C. M. Bitz and L.-B.
17 Tremblay), American Geophysical Union, Washington, D.C.. doi: 10.1029/180GM06, 2008

18 Boeke, R. C. and Taylor, P. C.: Evaluation of the Arctic surface radiation budget in CMIP5 models, *J. Geophys.*
19 *Res. Atmos.*, 121, 8525-8548, doi:10.1002/2016JD025099, 2016

20 Christensen, M. W., Behrangi, A., L'ecuyer, T. S., Wood, N. B., Lebsock, M. D. and Stephens, G. L.: Arctic
21 Observation and Reanalysis Integrated System: A New Data Product for Validation and Climate Study, *B. Am.*
22 *Meteorol. Soc.*, 97, 6, 907–916, doi: <https://doi.org/10.1175/BAMS-D-14-00273.1>, 2016

23 Collins, W. J., Bellouin, N., Doutriaux-Boucher, M., Gedney, N., Halloran, P., Hinton, T., Hughes, J., Jones, D.,
24 Joshi, M., Liddicoat, S., Martin, G., O'Connor, F., Rae, J., Senior, C., Sitch, S., Totterdell, I., Wiltshire, A. and
25 Woodward, S.: Development and evaluation of an Earth-System model – HadGEM2. *Geosci. Model Dev.*, 4,
26 1051-1075. doi:10.5194/gmd-4-1051-2011, 2011

27 Dee, D. P., Uppala, S. M., Simmons, A. J., Berrisford, P., Poli, P., Kobayashi, S., Andrae, U., Balmaseda, M. A.,
28 Balsamo, G., Bauer, P., Bechtold, P., Beljaars, A. C. M., van de Berg, L., Bidlot, J., Bormann, N., Belsol, C.,
29 Dragani, R., Fuentes, M., Geer, A., J., Haimberger, L., Healy, S. B., Hersbach, H., Holm, E. V., Isaksen, L.,
30 Kållberg, P., Köhler, M., Matricardi, M., McNally, A. P., Monge-Sanz, B. M., Morcrette, J.-J., Park, B.-K.,
31 Peubey, C., de Rosnay, P., Tavolato, C., Thépaut, J.-N. and Vitart, F.: The ERA-Interim reanalysis:
32 configuration and performance of the data assimilation system. *Quarterly Journal of the RMS* 137:553:597. doi:
33 10.1002/qj.828, 2011

34 DeWeaver, E. T., Hunke, E. C. and Holland, M. M.: Sensitivity of Arctic Sea Ice Thickness to Intermodel
35 Variations in the Surface Energy Budget. *AGU Geophysical Monograph* 180: Arctic Sea Ice Decline:
36 *Observations, Projections, Mechanisms and Implications*, 77-91. doi: 10.1029/180GM07, 2008

37 Gultepe, I., Isaac, G. A., Williams, A., Marcotte, D. and Strawbridge, K. B., Turbulent heat fluxes over leads
38 and polynyas, and their effects on arctic clouds during FIRE.ACE: Aircraft observations for April 1998,
39 *Atmosphere-Ocean*, 41:1, 15-34, DOI: 10.3137/ao.410102, 2003

40 [Holland, M.M., Serreze, M.C. and Stroeve, J., The sea ice mass budget of the Arctic and its future change as](#)
41 [simulated by coupled climate models, *Clim Dyn* \(2010\) 34: 185. doi:10.1007/s00382-008-0493-4](#)

Formatted: Font: (Default) +Body, 11 pt

- 1 Hunke, E. C. and Dukowicz, J. K., An Elastic–Viscous–Plastic Model for Sea Ice Dynamics, *J. Phys.*
2 *Oceanogr.*, 27, 9, 1849–1867, doi: [https://doi.org/10.1175/1520-0485\(1997\)027<1849:AEVPMF>2.0.CO;2](https://doi.org/10.1175/1520-0485(1997)027<1849:AEVPMF>2.0.CO;2),
3 1997.
- 4 Johns, T. C., Durman, C. F., Banks, H. T., Roberts, M. J., McLaren, A. J., Ridley, J. K., Senior, C. A., Williams,
5 K. D., Jones, A., Rickard, G. J., Cusack, S., Ingram, W. J., Crucifix, M., Sexton, D. M. H., Joshi, M. M., Dong,
6 B.-W., Spencer, H., Hill, R. S. R., Gregory, J. M., Keen, A. B., Pardaens, A. K., Lowe, J. A., Bodas-Salcedo, A.,
7 Stark, S. and Searl, Y.: The New Hadley Centre Climate Model (HadGEM1): Evaluation of Coupled
8 Simulations. *J Clim* 19:1327-1353. doi: 10.1175/JCLI3712.1, 2006
- 9 [Keen, A. B., Blockley, E., Investigating future changes in the volume budget of the Arctic sea ice in a coupled](https://doi.org/10.5194/tc-12-2855-2018)
10 [climate model. *The Cryosphere*, 12, 2855-2868, doi: 10.5194/tc-12-2855-2018, 2018.](https://doi.org/10.5194/tc-12-2855-2018)
- 11 Laxon, S., Peacock, N. and Smith, D.: High interannual variability of sea ice thickness in the Arctic region.
12 *Nature*, 425, 947-950, doi:10.1038/nature02050, 2003
- 13 Laxon, S., Giles, K. A., Ridout, A., Wingham, D. J., Willatt, R., Cullen, R., Kwok, R., Schweiger, A., Zhang, J.,
14 Haas, C., Hendricks, S., Krishfield, R., Kurtz, N., Farrell, S. and Davidson, M.: Cryosat-2 estimates of Arctic
15 sea ice thickness and volume. *Geophys Res Lett* 40:732-737. doi: 10.1002/grl.50193, 2013
- 16 Lindsay, R., Wensnahan, M., Schweiger, A. and Zhang, J.: Evaluation of Seven Difference Atmospheric
17 Reanalysis Products in the Arctic, *J. Clim.*, 27, 2588-2606, oi: 10.1175/JCLI-D-13-00014.1, 2013.
- 18 Lindsay, R. and Schweiger, A.: Arctic sea ice thickness loss determined using subsurface, aircraft, and satellite
19 observations. *The Cryosphere*, 9, 269-283. doi: 10.5194/tc-9-269-2015, 2015
- 20 Lipscomb, W. H. and Hunke, E. C., Modeling Sea Ice Transport Using Incremental Remapping, *Mon. Weather*
21 *Rev.*, 132, 6, 1341–1354, doi: [https://doi.org/10.1175/1520-0493\(2004\)132<1341:MSITUI>2.0.CO;2](https://doi.org/10.1175/1520-0493(2004)132<1341:MSITUI>2.0.CO;2), 2004
- 22 Liu, J., J. A. Curry, Rossow, W. B., Key, J. R. and Wang, X.: Comparison of surface radiative flux data sets
23 over the Arctic Ocean. *J. Geophys. Res.: Oceans*, 110, C2, doi: 10.1029/2004JC002381, 2005
- 24 Loeb, N. G., Wielicki, B. A., Doelling, D. R., Louis Smith, G., Keyes, D. F., Kato, S., Manalo-Smith, N. and
25 Wong, T.: Toward Optimal Closure of the Earth's Top-of-Atmosphere Radiation Budget. *J Cli*, 22, 3, 748–766.
26 doi: 10.1175/2008JCLI2637.1, 2009
- 27 Markus, T., Stroeve, J. C. and Miller, J.: Recent changes in Arctic sea ice melt onset, freezeup, and melt season
28 length. *J. Geophys. Res.*, 114, C12024. doi: 10.1029/2009JC005436, 2009
- 29 Martin, G. M., Bellouin, N., Collins, W. J., Culverwell, I. D., Halloran, P. R., Hardiman, S. C., Hinton, T. J.,
30 Jones, C. D., McDonald, R. E., McLaren, A. J., O'Connor, F. M., Roberts, M. J., Rodriguez, J. M., Woodward,
31 S., Best, M. J., Brooks, M. E., Brown, A. R., Butchart, N., Dearden, C., Derbyshire, S. H., Dharssi, I.,
32 Doutriaux-Boucher, M., Edwards, J. M., Falloon, P. D., Gedney, N., Gray, L. J., Hewitt, H. T., Hobson, M.,
33 Huddleston, M. R., Hughes, J., Ineson, S., Ingram, W. J., James, P. M., Johns, T. C., Johnson, C. E., Jones, A.,
34 Jones, C. P., Joshi, M. M., Keen, A. B., Liddicoat, S., Lock, A. P., Maidens, A. V., Manners, J. C., Milton, S. F.,
35 Rae, J. G. L., Ridley, J. K., Sellar, A., Senior, C. A., Totterdell, I. J., Verhoef, A., Vidale, P. L. and Wiltshire,
36 A., The HadGEM2 family of Met Office Unified Model climate configurations, *Geosci. Model Dev.*, 4, 723-
37 757, doi: <https://doi.org/10.5194/gmd-4-723-2011>, 2011
- 38 Maslanik, J., Stroeve, J. C., Fowler, C. and Emery, W.: Distribution and trends in Arctic sea ice age through
39 spring 2011. *Geophys. Res. Lett.*, 38, 47735. doi: 10.1029/2011GL047735, 2011
- 40 Massonnet, F., Fichefet, T., Goosse, H., Bitz, C. M., Philippon-Berthier, G., Holland, M. M. and Barriat, P.-Y.:
41 Constraining projections of summer Arctic sea ice, *The Cryosphere*, 6, 1383–1394, doi: 10.5194/tc-6-1383-
42 2012, 2012

- 1 Maykut, G. A. and McPhee, M. G., Solar heating of the Arctic mixed layer, *J. Geophys. Res.*, 100, C12, 24,691-
2 24,703, doi: 10.1029/95JC02554, 1995
- 3 McLaren, A. J., Banks, H. T., Durman, C. F., Gregory, J. M., Johns, T. C., Keen, A. B., Ridley, J. K., Roberts,
4 M. J., Lipscomb, W. H., Connolley, W. M. and Laxon, S. W.: Evaluation of the sea ice simulation in a new
5 coupled atmosphere-ocean climate model (HadGEM1). *J. Geophys. Res.*, 111, C12014. doi:
6 10.1029/2005JC003033, 2006
- 7 McPhee, M. G., Kikuchi, T., Morison, J. H. and Stanton, T. P.: Ocean-to-ice heat flux at the North Pole
8 environmental observatory, *Geophys. Res. Lett.*, 30, 2274, doi:10.1029/2003GL018580, 2003
- 9 Notz, D.: How well must climate models agree with observations?. *Philos T Roy Soc A*, 373, 2052. doi:
10 10.1098/rsta.2014.0164, 2015
- 11 Perovich, D. K. and Elder, B., Estimates of ocean heat flux at SHEBA, *Geophys. Res. Lett.*, 299, 9, 58-1 – 51-4,
12 doi: 10.1029/2001GL014171, 2002
- 13 Perovich, D. K., Richter-Menge, J. A., Jones, K. F. and Light, B.: Sunlight, water, and ice: Extreme Arctic sea
14 ice melt during the summer of 2007. *Geophys. Res. Lett.*, 35, 11. doi: 10.1029/2008GL034007, 2008
- 15 Pithan, F., Medeiros, B. and Mauritsen, T.: Mixed-phase clouds cause climate model biases in Arctic wintertime
16 temperature inversions, *Clim. Dyn.*, 43, 289-303, doi:10.1007/s00382-013-1964-9, 2014
- 17 Raddatz, R. L., Papakyriakou, T. N., Else, B. G., Asplin, M. G., Candlish, L. M., Galley, R. J. and Barber, D.
18 G.: Downwelling longwave radiation and atmospheric winter states in the western maritime Arctic. *Int. J. Clim.*,
19 35, 9, 2339-2351. doi: 10.1002/joc.4149, 2014
- 20 Rayner, N. A., Parker, D. E., Horton, E. B., Folland, C. K., Alexander, L. V., Rowell, D. P., Kent, E. C. and
21 Kaplan, A.: Global analyses of sea surface temperature, sea ice, and night marine air temperature since the late
22 nineteenth century. *J Geophys Res* 108:4407. doi:10.1029/2002JD002670, 2003
- 23 Rothrock, D. A., Percival, D. B. and Wensnahan, M.: The decline in arctic sea ice thickness: Separating the
24 spatial, annual, and interannual variability in a quarter century of submarine data. *J. Geophys. Res.*, 113,
25 C05003. doi: 10.1029/2007JC004252, 2008
- 26 Rutan, D. A., Kato, S., Doelling, D. R., Rose, F. G., Nguyen, L. T., Caldwell, T. E. and Loeb, N. G.: CERES
27 Synoptic Product: Methodology and Validation of Surface Radiant Flux, *J. Atmos. Ocean. Tech.*, 32(6), 1121-
28 1143. <http://dx.doi.org/10.1175/JTECH-D-14-00165.1>, 2015
- 29 [Schauer, U., Fahrbach, E., Osterhus, S. and Rohardt, G.: Arctic warming through Fram Strait: Oceanic heat
30 transport from 3 years of measurements, *J. Geophys. Res. \(Oceans\)*, 109, C6, doi: 10.1029/2003JC001823,
31 2004.](#)
- 32 Schweiger, A. J., Lindsay, R. W., Zhang, J., Steele, M. and Stern, H.: Uncertainty in modeled arctic sea ice
33 volume, *J. Geophys. Res.*, doi:10.1029/2011JC007084, 2011
- 34 Semtner, A. J.: A Model for the Thermodynamic Growth of Sea Ice in Numerical Investigations of Climate. *J.*
35 *Phys. Oceanogr.*, 6, 3, 379–389. doi: 10.1175/1520-0485, 1976.
- 36 Serreze, M. C., Barrett, A. P., Slater, A. G., Woodgate, R. A., Aagaard, K., Lammers, R. B., Steele, M., Moritz,
37 R., Meredith, M. and Lee, C. M.: The large-scale freshwater cycle of the Arctic, *J. Geophys. Res.*, 111, C11010,
38 doi:10.1029/2005JC003424, 2006
- 39 Shu, Q., Song, Z. and Qiao, F. (2015) Assessment of sea ice simulation in the CMIP5 models. *The Cryosphere*,
40 9, 399–409. doi: 10.5194/tc-9-399-2015

- 1 | [Stammerjohn, S., Massom, R., Rind, D. and Martinson, D.: Regions of rapid sea ice change: An](#)
2 | [inter-hemispheric seasonal comparison, *Geophys. Res. Lett.*, 39, 6. doi: 10.1029/2012GL050874, 212](#)
- 3 | Stramler, K., Del Genio, A. D. and Rossow, W. B.: Synoptically Driven Arctic Winter States. *J. Clim.*, 24,
4 | 1747–1762. doi: 10.1175/2010JCLI3817.1, 2011
- 5 | [Steele, M. Zhang, J.; Ermold, W.: Mechanisms of summer Arctic Ocean warming, *J. Geophys. Res. \(Oceans\)*,](#)
6 | [115, C11, doi: 10.1029/2009JC005849 \(2010\)](#)
- 7 | Stroeve, J. C., Kattsov, V, Barrett, A., Serreze, M., Pavlova, T., Holland, M. M. and Meier, W. N.: Trends in
8 | Arctic sea ice extent from CMIP5, CMIP3 and observations. *Geophys. Res. Lett.*, 39, doi:
9 | 10.1029/2012GL052676, 2012a.
- 10 | Stroeve, J. C., Serreze, M. C., Holland, M. M., Kay, J. E., Maslanik, J., Barratt, A. P.: The Arctic’s rapidly
11 | shrinking sea ice cover: a research synthesis, *Clim. Ch.*, 110, 1005–1027, doi: [https://doi.org/10.1007/s10584-](https://doi.org/10.1007/s10584-011-0101-1)
12 | [011-0101-1](https://doi.org/10.1007/s10584-011-0101-1), 2012b
- 13 | Swart, N. C., Fyfe, J. C., Hawkins, E., Kay, J. E. and Jahn, A.: Influence of internal variability on Arctic sea ice
14 | trends, *Nat. Clim. Ch.*, 5, 86–89, doi:10.1038/nclimate2483, 2015
- 15 | Thorndike, A. S., Rothrock, D. A., Maykut, G. A. and Colony, R., The thickness distribution of sea ice, *J.*
16 | *Geophys. Res.*, 80, 4501-4513, doi: 10.1029/JC080i033p04501, 1975
- 17 | Tsamados, M., Feltham, D. L. and Wilchinsky, A. V., Impact of a new anisotropic rheology on simulations of
18 | Arctic sea ice, *J. Geophys. Res. – Oceans*, 118, 1, 91-107, doi: 10.1029/2012JC007990, 2013
- 19 | Wang, M. and Overland, J. E.: A sea ice free summer Arctic within 30 years? *Geophys. Res. Lett.*, , 36,
20 | L07502, doi:10.1029/2009GL037820, 2009
- 21 | Wang, X., Key, J., Kwok, R. and Zhang, J.: Comparison of Arctic Sea Ice Thickness from Satellites, Aircraft
22 | and PIOMAS data, *Remote Sens.*, 8(9), 713; doi:[10.3390/rs8090713](https://doi.org/10.3390/rs8090713), 2016
- 23 | Zhang, Y., Rossow, W. B., Lacis, A. A., Oinas, V., and Mishchenko, M. I.: Calculation of radiative fluxes from
24 | the surface to top of atmosphere based on ISCCP and other global data sets: Refinements of the radiative
25 | transfer model and the input data, *J. Geophys. Res.*, 109, D19105, doi:10.1029/2003JD004457, 2004
- 26 |
27 |

<u>Month</u>	<u>Downwelling SW</u>	<u>Downwelling LW</u>	<u>Ice thickness</u>	<u>Ice area</u>	<u>Melt onset occurrence</u>	<u>Total induced surface flux bias</u>	<u>Radiative flux bias</u>	<u>ISF residual</u>	<u>CERES-ERA1 net radiation difference</u>
<u>Jan</u>	<u>0.0</u>	<u>-6.5</u>	<u>-4.3</u>	<u>2.7</u>	<u>0.0</u>	<u>-8.1</u>	<u>-1.6</u>	<u>3.3</u>	<u>-12.2</u>
<u>Feb</u>	<u>0.0</u>	<u>-4.8</u>	<u>-2.8</u>	<u>2.3</u>	<u>0.0</u>	<u>-5.3</u>	<u>-10.4</u>	<u>4.6</u>	<u>-12.5</u>
<u>Mar</u>	<u>0.1</u>	<u>-3.8</u>	<u>-2.0</u>	<u>2.0</u>	<u>0.0</u>	<u>-3.7</u>	<u>-10.5</u>	<u>5.9</u>	<u>-12.0</u>
<u>Apr</u>	<u>0.4</u>	<u>-4.4</u>	<u>-1.4</u>	<u>1.4</u>	<u>0.2</u>	<u>-4.2</u>	<u>-12.2</u>	<u>7.6</u>	<u>-9.7</u>
<u>May</u>	<u>2.1</u>	<u>-4.8</u>	<u>-0.6</u>	<u>0.0</u>	<u>0.1</u>	<u>-3.2</u>	<u>-3.7</u>	<u>0.5</u>	<u>-3.5</u>
<u>Jun</u>	<u>-8.3</u>	<u>7.4</u>	<u>0.0</u>	<u>1.7</u>	<u>11.4</u>	<u>12.2</u>	<u>27.8</u>	<u>-15.4</u>	<u>-4.2</u>
<u>Jul</u>	<u>-13.6</u>	<u>8.0</u>	<u>0.0</u>	<u>3.7</u>	<u>3.3</u>	<u>1.4</u>	<u>5.1</u>	<u>-3.9</u>	<u>-16.9</u>
<u>Aug</u>	<u>0.5</u>	<u>-3.3</u>	<u>-0.1</u>	<u>9.6</u>	<u>1.9</u>	<u>8.5</u>	<u>8.6</u>	<u>-0.0</u>	<u>-12.9</u>
<u>Sep</u>	<u>3.3</u>	<u>-7.1</u>	<u>-0.7</u>	<u>-0.7</u>	<u>0.0</u>	<u>-5.2</u>	<u>-0.2</u>	<u>-4.8</u>	<u>-2.4</u>
<u>Oct</u>	<u>0.9</u>	<u>-5.7</u>	<u>-4.2</u>	<u>-1.8</u>	<u>0.0</u>	<u>-10.8</u>	<u>-14.4</u>	<u>3.4</u>	<u>-4.6</u>
<u>Nov</u>	<u>0.0</u>	<u>-5.4</u>	<u>-8.3</u>	<u>-0.3</u>	<u>0.0</u>	<u>-14.0</u>	<u>-21.6</u>	<u>8.1</u>	<u>-11.7</u>
<u>Dec</u>	<u>0.0</u>	<u>-6.4</u>	<u>-6.4</u>	<u>2.4</u>	<u>0.0</u>	<u>-10.4</u>	<u>-14.9</u>	<u>4.1</u>	<u>-12.2</u>

1 Table 1. Surface flux biases induced by model bias in 5 different variables in HadGEM2-ES (Wm^{-2}), with
2 CERES used as reference dataset for the radiative components. Total ISF bias and total net radiative flux bias
3 relative to CERES are shown for comparison, as well as their residual; the difference between net radiative flux
4 bias as evaluated by CERES and ERA1 is also shown. A positive number denotes a downwards flux, and vice
5 versa.

Formatted: Superscript

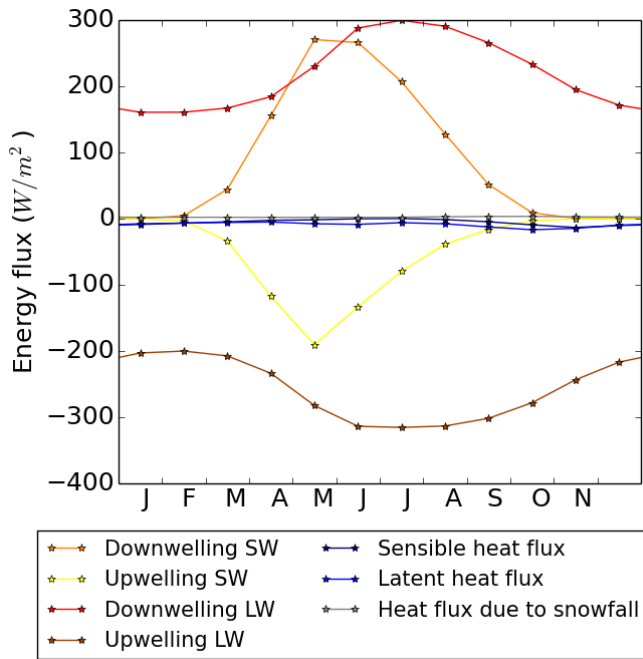


Formatted: Font: (Default) Times New Roman, 9 pt, Bold

1

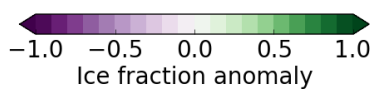
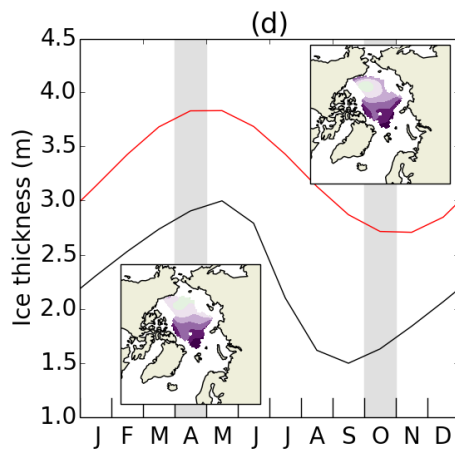
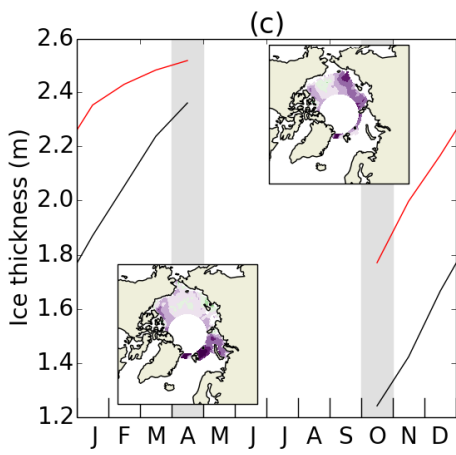
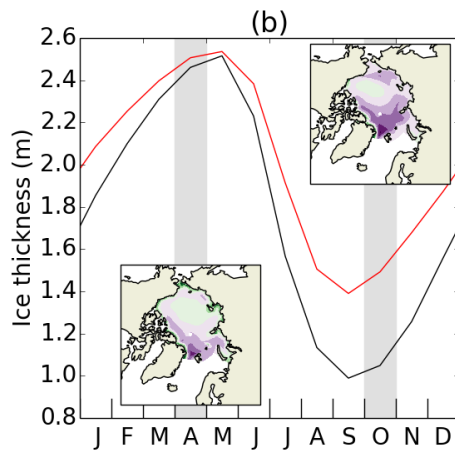
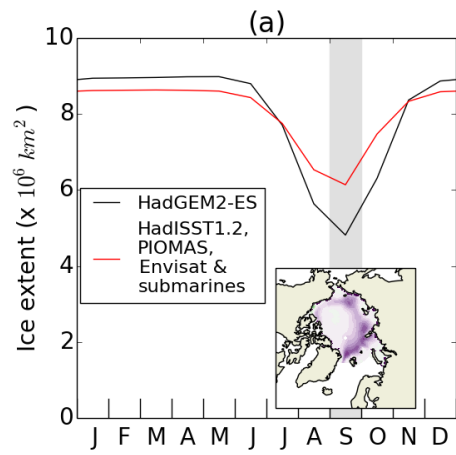
2 **Figure 1. The Arctic Ocean region used in the analysis.**

3



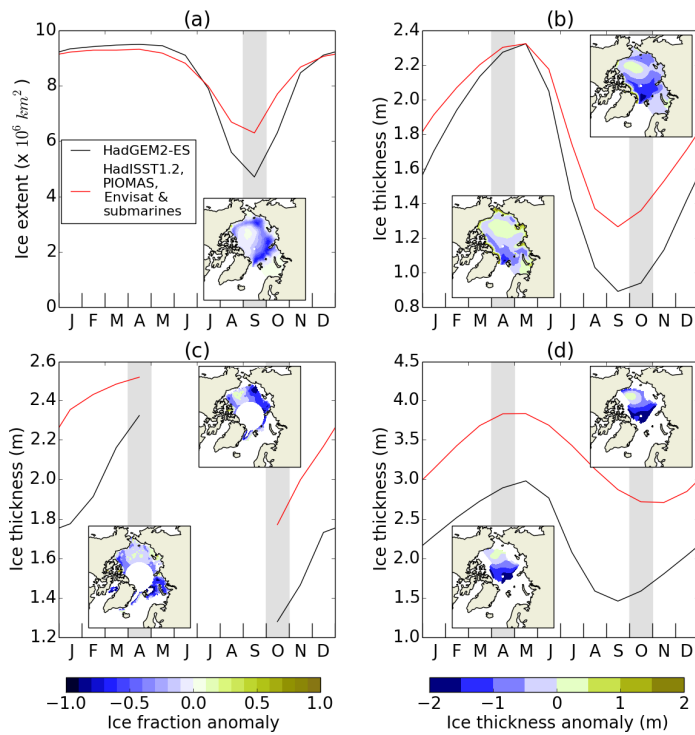
Formatted: Font: (Default) Times New Roman, 9 pt, Bold

1
2 **Figure 2. 1980-1999 mean surface fluxes over the Arctic Ocean region for the first historical run of HadGEM2-ES.**



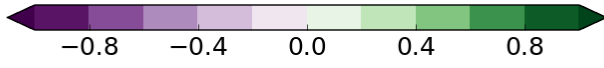
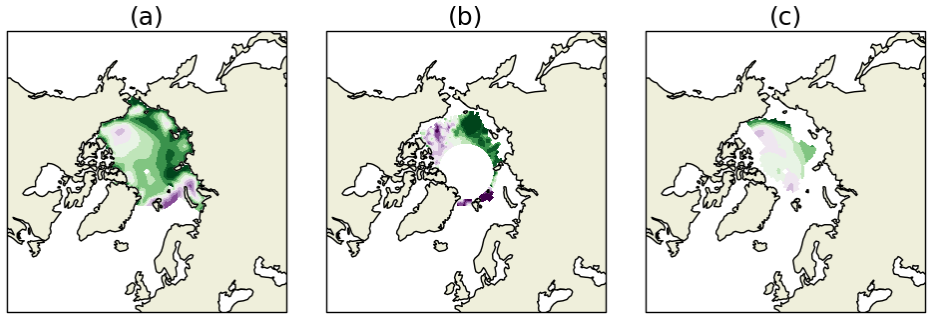
Formatted: Font: (Default) Times New Roman, 9 pt, Bold

1

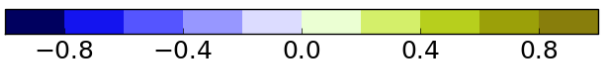
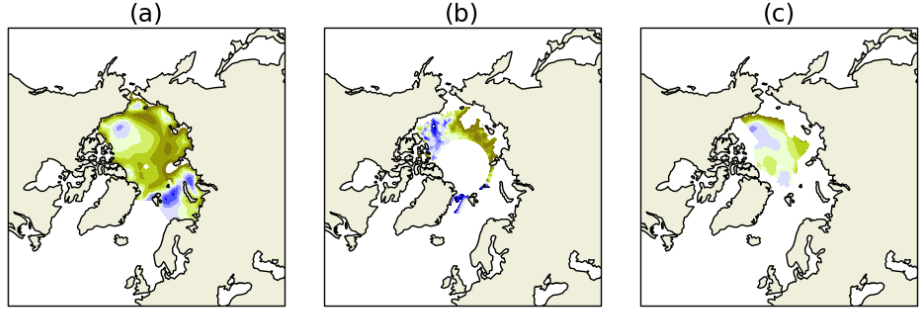


1 .
 2 **Figure 23.** (a) HadGEM2-ES 1980-1999 mean Arctic Ocean ice extent, compared to HadISST1.2 1980-1999, with
 3 September ice fraction **bias anomaly**-map; (b-d) HadGEM2-ES 1980-1999 ice thickness compared to (b) PIOMAS, (c)
 4 Envisat and (d) submarine datasets over respective regions of coverage, with April and October ice thickness **bias**
 5 **anomaly**-maps. For each seasonal cycle plot, the model is in black and observations in red. In (c), data is not plotted
 6 from May-September due to the region of coverage being very small.

7



Model anomaly in October-April thickness change (m)



Model anomaly in October-April thickness change (m)

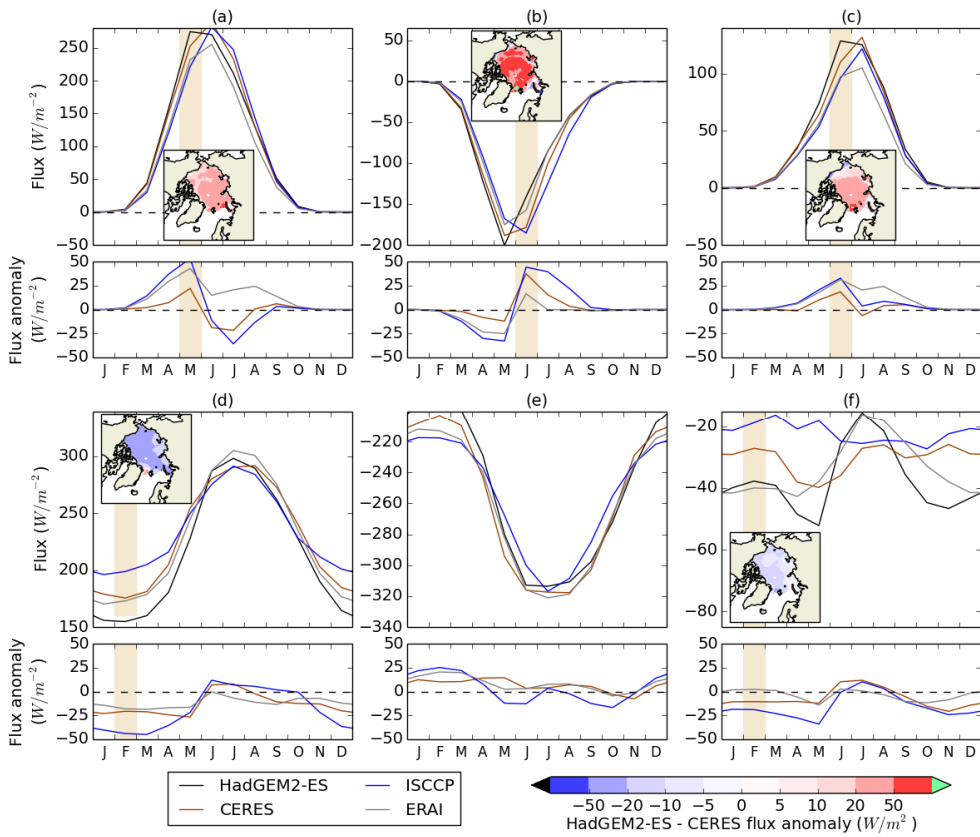
Formatted: Font: (Default) Times New Roman, 9 pt, Bold

1
2
3
4
5
6
7

Figure 34. HadGEM2-ES 1980-1999 model bias anomaly in ice thickness change from October-April compared to (a) PIOMAS 1980-1999; (b) Envisat 1993-2000; (c) submarine regression analysis 1980-1999. Differences are taken as model-observation so that areas of green (purple) correspond to areas where the HadGEM2-ES model simulates too much (not enough) sea ice growth through the winter

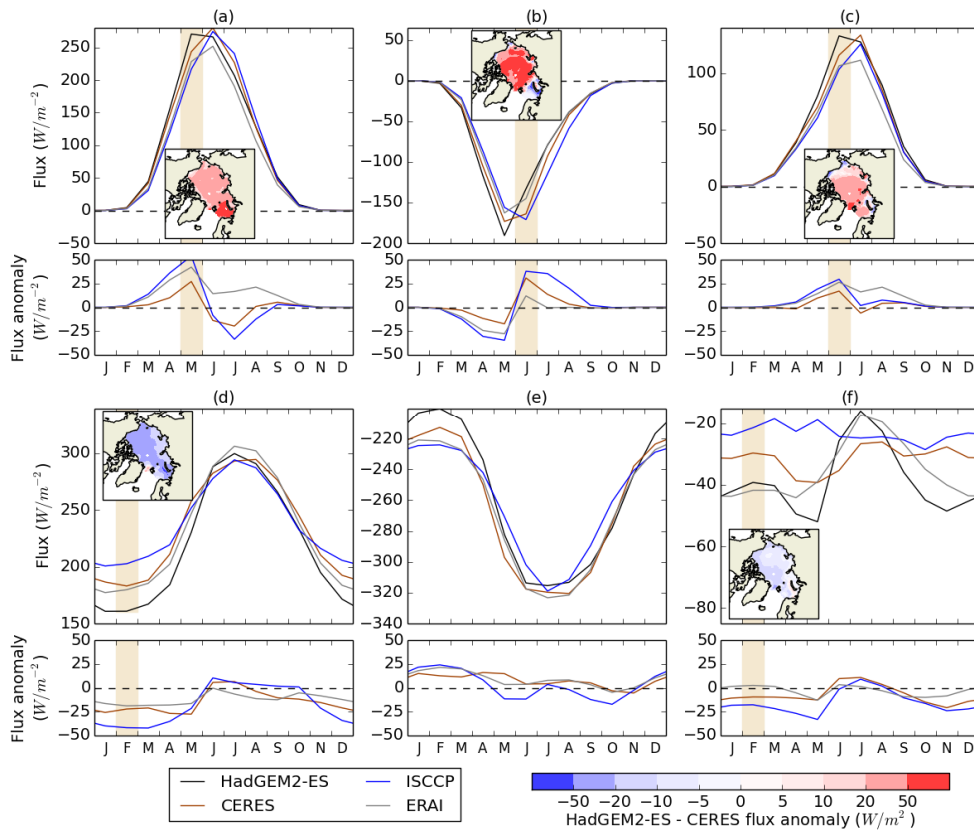
Formatted: Font: 10 pt

Formatted: Font: (Default) Times New Roman, 10 pt, Bold



Formatted: Font: (Default) Times New Roman, 9 pt, Bold

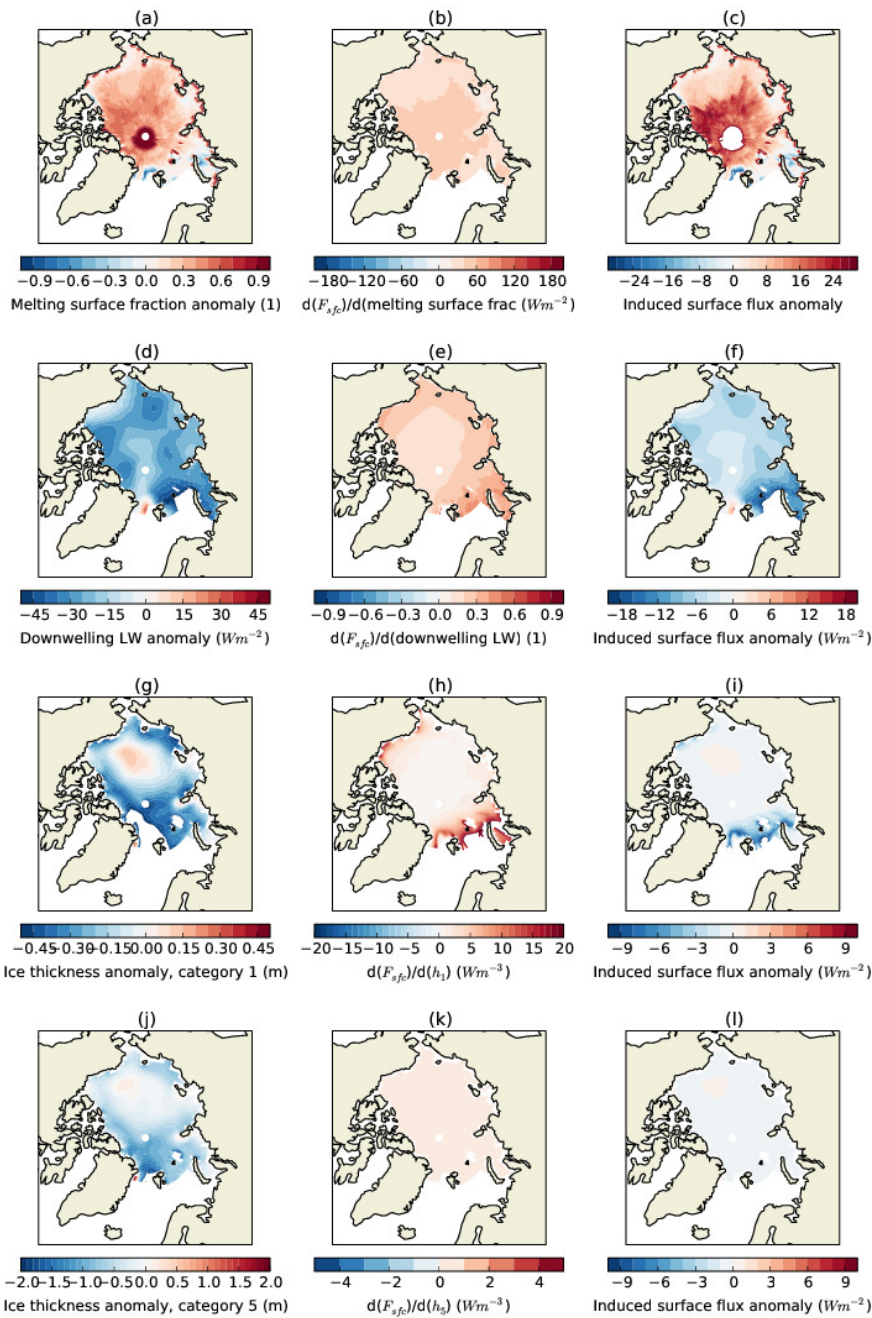
1



1
 2 **Figure 45.** (a) Downwelling SW, (b) upwelling SW, (c) net down SW, (d) downwelling LW, (e) upwelling LW, (f) net
 3 down LW, for HadGEM2-ES 1980-1999 over the Arctic Ocean region, compared to CERES 2000-2013, ISCCP-D
 4 1983-1999 and ERAI 1980-1999. For all fluxes, a positive number denotes a downward flux and vice versa. Maps of
 5 flux **bias anomaly** relative to CERES are shown for downwelling SW in May, upwelling and net down SW in June,
 6 and downwelling and net down LW in February.

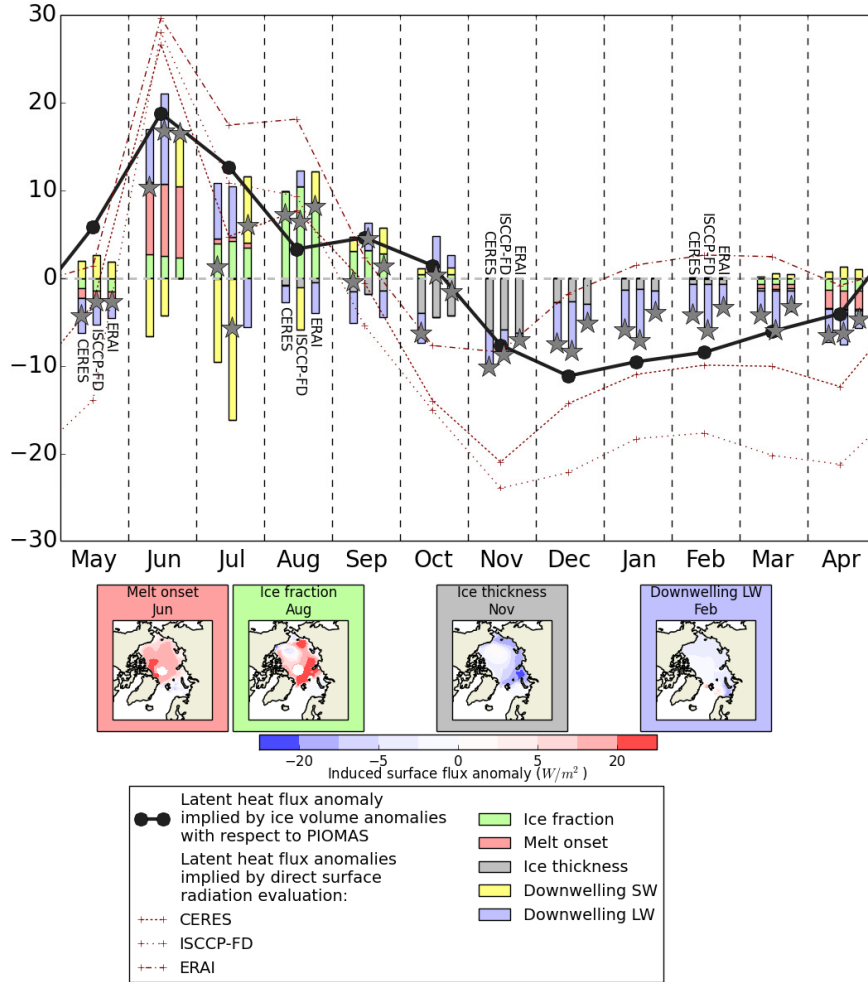
7

Formatted: Font: (Default) Times New Roman, 9 pt, Bold



1
2 **Figure 5. Demonstrating the calculation of fields of surface flux bias due to model bias in melting surface**
3 **fraction (a-c), downwelling LW (d-f), category 1 ice thickness (g-i) and category 5 ice thickness (j-l). The**
4 **left-hand column shows model bias in each variable; the middle column the local rate of dependence of**
5 **surface flux on each variable as calculated above; the right column the induced surface flux bias,**
6 **calculated as the product of these two fields.**

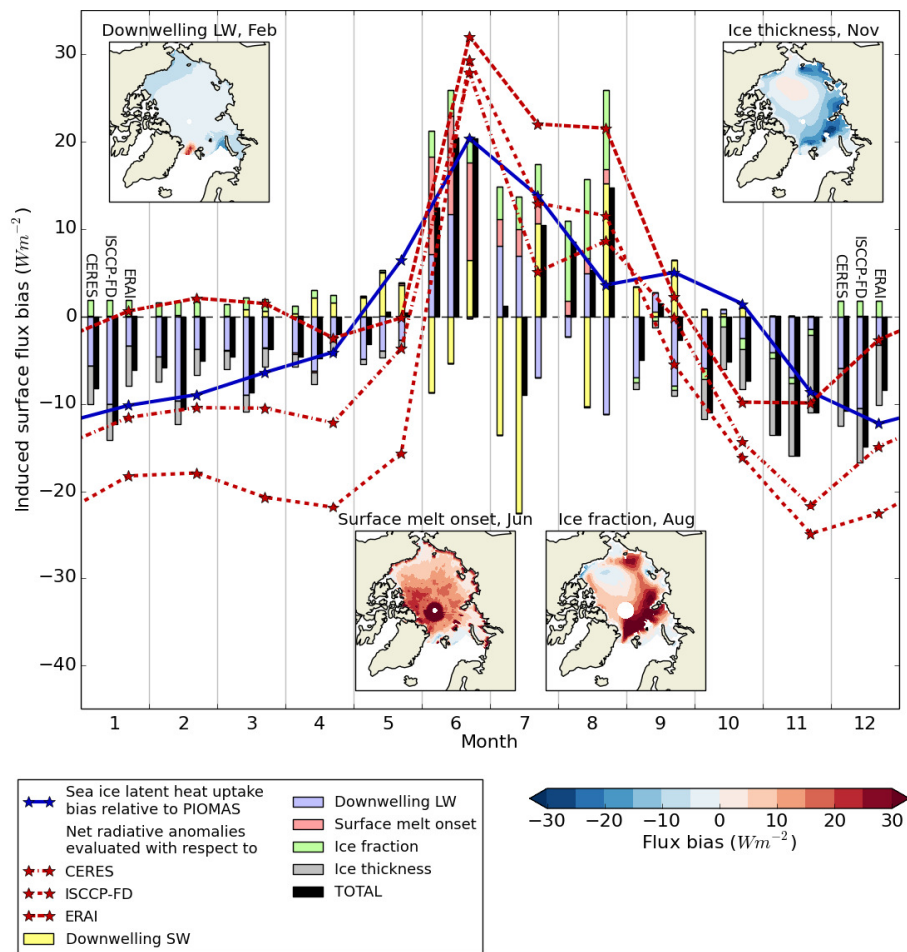
1



Formatted: Font: (Default) Times New Roman, 9 pt, Bold

2

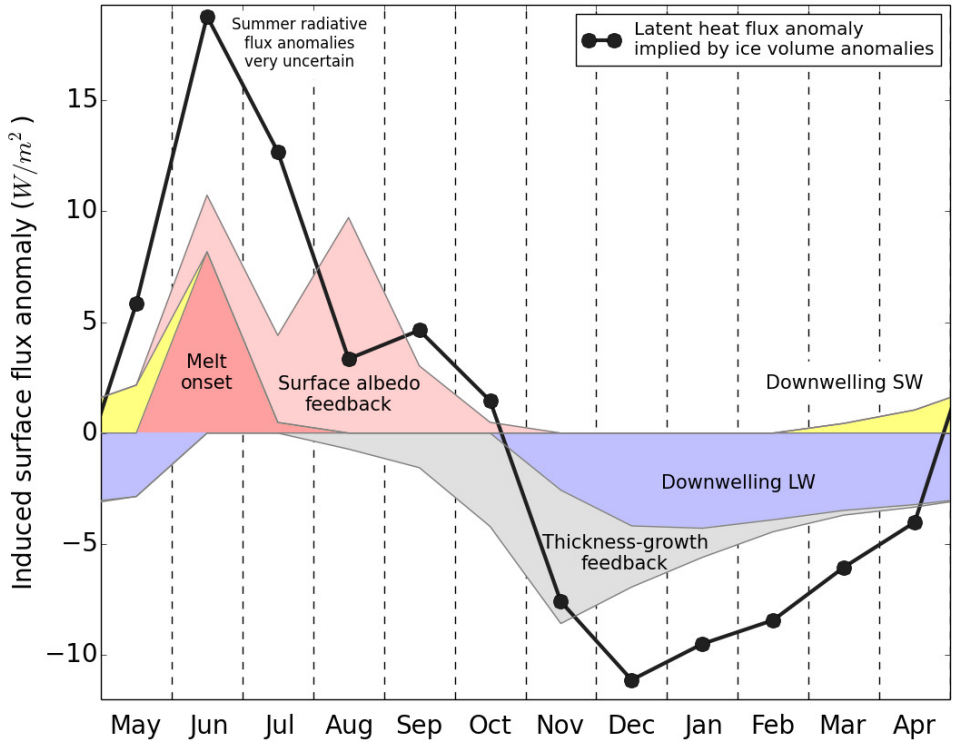
3 **Figure 6. Surface flux anomaly induced by model anomalies in ice fraction, melt onset occurrence, ice thickness,**
 4 **downwelling SW and downwelling LW respectively, for the Arctic Ocean region in HadGEM2-ES, 1980-1999, as**
 5 **estimated by the simple models described in Section 2.3. For each month, induced anomalies are estimated using in**
 6 **turn CERES, ISCCP-FD and ERAI as radiation reference datasets, from left-right. Sea ice latent heat flux uptake**
 7 **anomaly relative to PIOMAS is indicated in black. Net radiative flux anomalies relative to CERES, ISCCP-FD and**
 8 **ERAI are indicated in brown. Spatial patterns of induced surface flux anomaly for four processes in key months,**
 9 **with CERES as reference dataset, are displayed beneath.**



Formatted: Font: (Default) Times New Roman, 10 pt

1
2
3
4
5
6
7
8
9
10

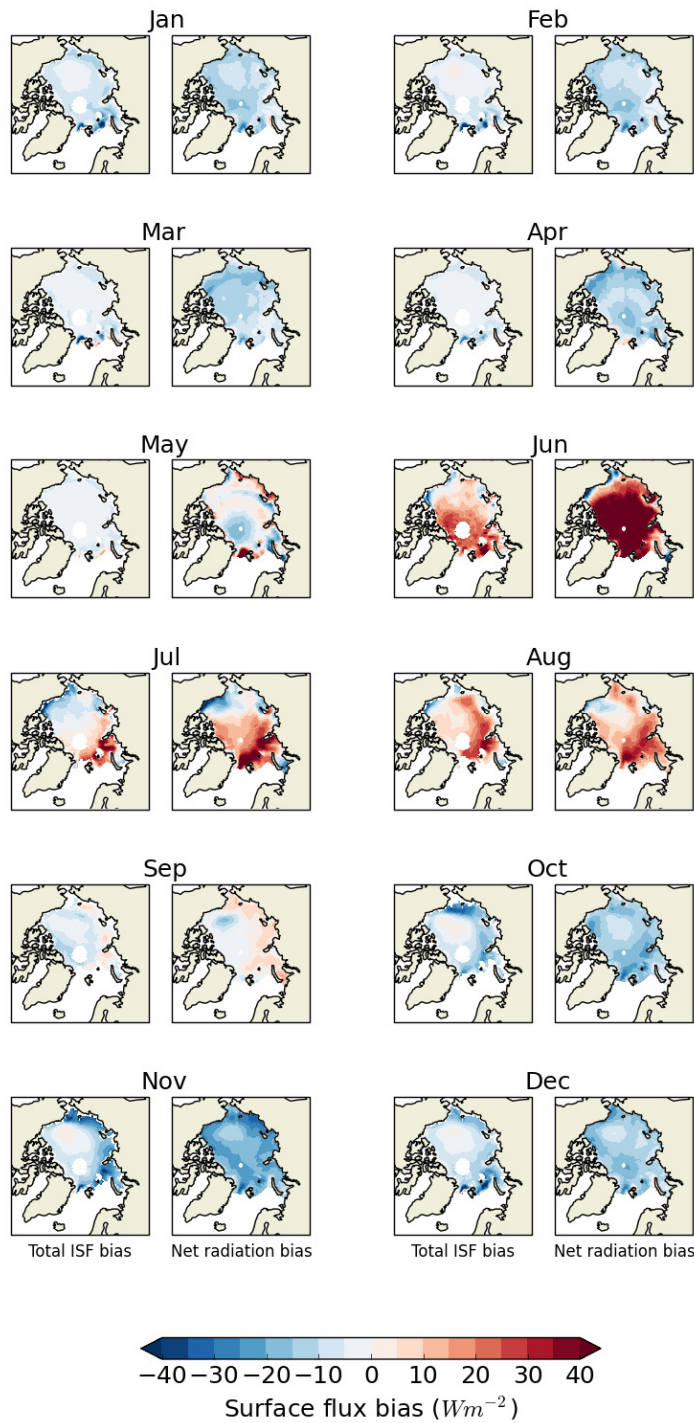
Figure 6. Surface flux bias induced by model biases in ice fraction, melt onset occurrence, ice thickness, downwelling SW and downwelling LW respectively, for the Arctic Ocean region in HadGEM2-ES, 1980-1999, as estimated by the simple models described in Section 2.3. For each month, induced surface flux biases are estimated using in turn CERES, ISCCP-FD and ERAI as radiation reference datasets, from left-right. Sea ice latent heat flux uptake bias relative to PIOMAS is indicated in black. Net radiative flux biases relative to CERES, ISCCP-FD and ERAI are indicated in brown. Spatial patterns of induced surface flux bias for four processes in key months, with CERES as reference dataset, are displayed beneath.



Formatted: Font: (Default) Times New Roman, 9 pt, Bold

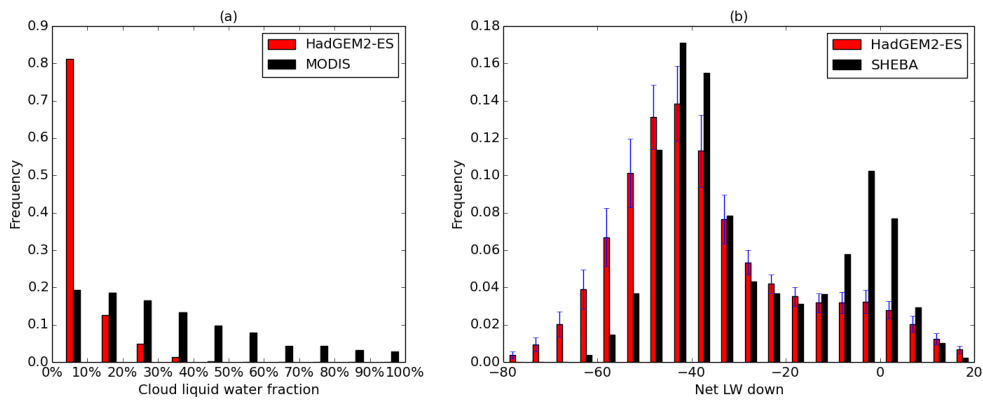
1
 2 **Figure 7. Surface flux anomalies caused by anomalies in external forcings, and to feedbacks due to anomalies in the**
 3 **sea ice state, represented as stacked filled regions. All values shown are means across radiation datasets shown in**
 4 **Figure 4; summer radiative flux anomalies are not plotted due to very large spread among datasets.**

Formatted: Font: (Default) Times New Roman, 9 pt, Bold



1
2
3

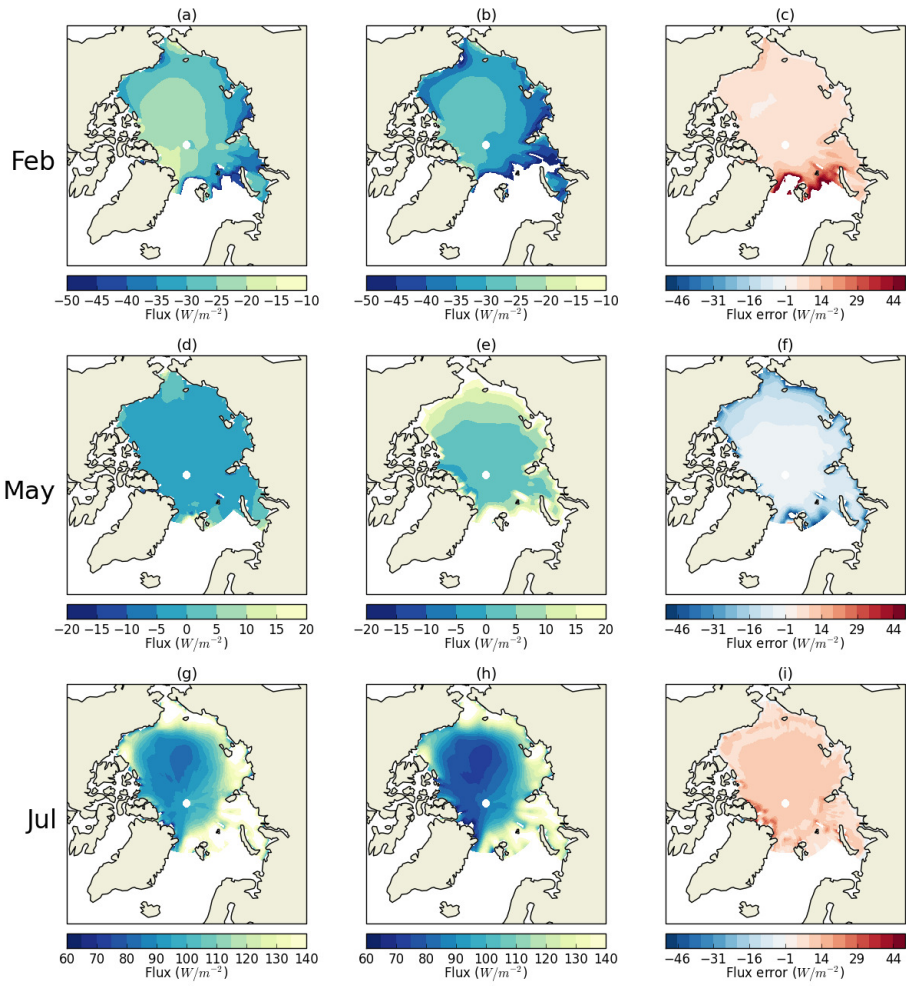
Figure 7. Comparing fields of total ISF bias to net radiation bias relative to CERES for each month of the year, for the four historical members of HadGEM2-ES, 1980-1999.



1
 2 **Figure 8. Frequency distributions of (a) October-April cloud liquid water percentage in HadGEM2-ES compared to**
 3 **MODIS observations, for the Arctic Ocean region; (b) December-February surface net downwelling LW in**
 4 **HadGEM2-ES in the SHEBA region, compared to the values observed at SHEBA.**

5

6



1
2 **Figure A1. Illustrating approximated (left) and actual (centre) model net surface flux, as well as the**
3 **approximation error (right), in (a-c) February; (d-f) May; (g-i) July, for the period 1980-1999 in the first**
4 **historical run of HadGEM2-ES.**

5